UNIVERSITY
OF MICHIGAN
JUN 24 1952
PHYSICS
LIBRARY

REGISTERED NO. M. 3121

PROCEEDINGS

OF THE

INDIAN ACADEMY

OF SCIENCES

VOL. XXXV] *SECTION A* [NO. 3

MARCH 1952

Price Rs. 2 or 3 Sh. *Annual Subscription Rs. 18*

PRINTED AT THE BANGALORE PRESS, BANGALORE CITY, BY G. SRINIVASA RAO,
SUPERINTENDENT, AND PUBLISHED BY THE INDIAN ACADEMY OF SCIENCES,
BANGALORE.

THE OPTICAL ROTATORY POWER OF QUARTZ AND ITS VARIATION WITH TEMPERATURE

By S. Chandrasekhar

(From the Raman Research Institute, Bangalore)

Received January 15, 1951
(Communicated by Sir C. V. Raman)

1. Introduction

Soon after the discovery of the optical activity of quartz by Arago in 1811, Biot showed that the magnitude of the rotation in the visible region of the spectrum is inversely proportional to the square of the wavelength, *i.e.*, $\rho = k/\lambda^2$. The rotary dispersion of quartz has been, subsequently, the subject of numerous investigations. These have been reviewed by Sosman in his book on the properties of silica (1927) and by Lowry in his treatise on optical rotatory power (1935). More recently, the measurements have been extended into the ultra-violet upto 1525 A.U. by Servant (1938) and into the infra-red upto $9{\cdot}7\,\mu$ by Gutowsky (1951). From these determinations it is evident that Biot's Law fails completely as we move away from the visible region of the spectrum in either direction. Indeed, in the ultra-violet, the rotatory power increases from 6000 A.U. to 1500 A.U. nearly 40 times instead of 16 times as required by the inverse square formula. Several attempts have been made to represent the rotary dispersion numerically in terms of various assumed dispersion frequencies. A critical examination of these formulæ, however, shows that they are arbitrary in character and do not possess any real physical justification.

A noteworthy fact about the optical rotatory power of quartz is that it increases appreciably when the temperature of the crystal is raised, the rate of increase accelerating as the temperature approaches that at which the α-β transformation in crystalline quartz takes place. At the transition point itself, there is an abrupt increment in the rotatory power. The temperature-coefficient remains positive in β-quartz but is very much smaller than in α-quartz. Though many experimental studies dealing with these effects are on record, no attempt appears to have been made to give a theoretical explanation of the influence of temperature on the optical activity of quartz.

It is proposed to discuss in this paper, firstly, the manner in which the optical rotatory power of quartz varies with wave-length and secondly, its

variation with the temperature of the crystal. It emerges from the discussion that the two topics are closely interrelated.

Other crystals, *viz.*, cinnabar and sodium chlorate, are known which are optically active and in which also the temperature coefficient of the optical rotatory power is positive. These cases will be discussed in later papers.

2. The Earlier Formulæ for the Rotary Dispersion

The first attempt at a theoretical formula to fit the rotary dispersion of quartz was made by Drude in his "Optics" where he proposed the form

$$\rho = \sum_r \frac{Q_r}{\lambda^2 - \lambda_r^2}, \tag{1}$$

where ρ is the optical rotatory power (in degrees per millimetre), Q_r is a constant corresponding to the characteristic absorption wavelength λ_r (in microns), the summation being performed over all the r absorption frequencies. Drude found that the then available data could be fitted by a two-term formula, where

$$Q_1 = 12{\cdot}2 \qquad Q_2 = -5{\cdot}046$$
$$\lambda_1^2 = 0{\cdot}010627 \qquad \lambda_2^2 = 0.$$

the negative term being unambiguously indicated to be necessary.

Since then several other modified formulæ have been suggested by various authors. Lowry (1912) noticed that Drude's formula is not accurate enough to fit his first series of extended measurements and hence altered it to

$$\rho = \frac{11{\cdot}6064}{\lambda^2 - 0{\cdot}010627} - \frac{4{\cdot}3685}{\lambda^2} + \frac{13{\cdot}42}{\lambda^2 - 78{\cdot}22} \tag{2}$$

the additional third term corresponding to the infra-red absorption band. His later still more accurate readings upto 2263 A.U. however required still further modification and his final formula is

$$\rho = \frac{9{\cdot}5639}{\lambda^2 - 0{\cdot}0127493} - \frac{2{\cdot}3113}{\lambda^2 - 0{\cdot}000974} - 0{\cdot}1905 \tag{3}$$

where instead of the single absorption band at 1031 A.U. occurring in the previous formulæ, two new characteristic wave-lengths 1129 A.U. and 312 A.U. have been used, the effect of the infra-red being substituted by a constant.

Neither of these latter formulæ, however, represent the results of Duclaux and Jeantet (1926) which extend upto 1854 A.U. and therefore another formula was worked out by Bradshaw and Livens (1929), *viz.*,

$$\rho = \frac{845{\cdot}694}{(\lambda^2 - 0{\cdot}01274912)} - \frac{0{\cdot}40235}{(\lambda^2 - 0{\cdot}01274912)^2}$$

$$- \frac{838{\cdot}4320}{(\lambda^2 - 0{\cdot}0120800)} - \frac{0{\cdot}1331233}{(\lambda^2 - 0{\cdot}0120800)^2} + \frac{43{\cdot}05794}{(\lambda^2 - 80{\cdot}00)}$$

$$+ \frac{2119{\cdot}117}{(\lambda^2 - 80{\cdot}00)^2}. \qquad (4)$$

It will be noticed that in this formula, the optical rotatory power is expressed as a difference of two very large terms of nearly equal magnitude but of opposite signs involving two close absorption wave-lengths respectively at 1129 A.U. and 1099 A.U., and that the influence of the infra-red term has been retained. Though some additional terms of a different type occur in this formula, it is clear that the terms of the Drude type appearing in it are the principal ones. The formula, however, gives values which deviate notably from the newer extended measurements of Servant (*loc. cit.*) in the remote ultra-violet. Radhakrishnan (1947) has therefore fitted these results with still another rotary dispersion formula, *viz.*,

$$\rho = \frac{4{\cdot}948}{\lambda^2 - 0{\cdot}014161} + \frac{4{\cdot}617}{\lambda^2 - 0{\cdot}011236} - \frac{2{\cdot}311}{\lambda^2 - 0{\cdot}000974}$$

$$- \frac{0{\cdot}000815}{(\lambda^2 - 0{\cdot}0195)^2} - 0{\cdot}1905 \qquad (5)$$

This formula is largely a refinement on the work of Lowry and Coode Adams. The absorption at 312 A.U. is still retained but the single term at 1129 A.U. has been split into two terms at 1060 A.U. and 1190 A.U. In addition, a small negative term at about 1400 A.U., almost at the very limit of continuous absorption in quartz has been introduced. This formula fits the entire data fairly well.

Thus, we see that a variety of formulæ involving numerous hypothetical absorption frequencies have been suggested to numerically represent the rotary dispersion of quartz. On examining these formulæ, we notice that, without exception, all the authors have been obliged to introduce negative terms involving absorption wave-lengths lying in the ultra-violet, in order to fit the data over the whole spectrum. No physical justification has been given for this procedure. The necessity for assigning a negative strength to a term becomes clear when we consider a single-term formula of the type (1) as suggested by Drude. When $\lambda_r = 0$, this reduces to Biot's Law. When λ_r takes finite values, the rotatory power varies faster with wave-length than required by Biot's Law. The rotatory power has been calculated for several wave-lengths giving various values to λ_r in this formula and shown in

Table I. These values of λ_r have been chosen at random over the entire region of continuous absorption in quartz which extends below 1436 A.U. (Tousey, 1940). In each column, the rotatory power has been fitted with the experimental value for $\lambda = 0{\cdot}6708\,\mu$. (Throughout, ρ is expressed in degrees per millimetre.)

TABLE I

Rotary dispersion using one-term formula of Drude type

λ (*in* μ)	ρ (Calculated)					ρ (Experimental)
	$\lambda_r = 0$	$\lambda_r = \cdot 03\mu$	$\lambda_r = \cdot 06\mu$	$\lambda_r = \cdot 10\mu$	$\lambda_r = \cdot 12\mu$	
·1525	320	332	375·6	549	813	776
·1625	281·8	291·2	323·7	443·5	600·0	599·5
·1825	223·4	229·1	248·5	312·2	381·0	391·5
·2359	133·7	135·6	141·8	159·4	174·6	180·4
·3728	53·5	53·8	54·5	56·4	57·8	58·8
·4678	34·0	34·1	34·3	34·8	35·2	35·6
·6708	16·54	16·54	16·54	16·54	16·54	16·54

It is seen that for all values of λ_r, except $\lambda_r = 1200$ A.U., the calculated rotatory power is much lower than the observed value over the whole range of wave-lengths. The same is true even for $\lambda_r = 1200$ A.U. except in the remote ultra-violet region where the calculations exceed the observed data. On a careful study of this table it can easily be understood why no combination of positive terms can ever accurately represent the rotary dispersion of quartz. For, even if at the two extremes of the spectrum the values be accurately fitted by a suitable choice of terms, there will be a large region in the visible and near ultra-violet for which the calculated values will be less than the experimental values. This difficulty has been overcome by the previous authors by expressing the rotatory power as a difference of two terms. Evidently, these formulæ are purely empirical in character and do not give a real explanation of the facts. Hence, we may conclude that a rotary dispersion formula of the type suggested by Drude is not appropriate in the case of quartz.

3. A NEW FORMULA

The present author has found that the rotary dispersion of quartz is accurately represented throughout the visible and ultra-violet range of the spectrum by a simple formula containing only two constants, *viz.*,

$$\rho = \frac{k\lambda^2}{(\lambda^2 - \lambda_0^2)^2} \qquad (6)$$

It is seen that the formula approximates to Biot's Law when $\lambda >> \lambda_0$. Also for a given value of λ_0, the rate of variation of the rotation with wavelength from this formula is much greater than from the Drude formula. The constants which fit the experimental data are

$$k = 7{\cdot}186 \text{ and } \lambda_0 = 0{\cdot}0926283\,\mu.$$

The rotatory power calculated from this formula are given in comparison with the experimental values in Table II.

TABLE II

Rotary dispersion using author's formula

λ (in μ)	ρ (experimental)	ρ (calculated)	λ (in μ)	ρ(experimental)	ρ (calculated)
·1525	776	776	·291216	104·97	104·88
·1575	724	724	·340365	72·46	72·35
·1625	599·5	597·2	·372762	58·84	58·75
·1675	533·0	531·5	·435834	41·55	41·50
·1700	504·5	503·0	·467816	35·61	35·57
·1750	453·5	452·8	·479991	33·68	33·65
·1775	431·5	430·7	·508582	29·73	29·72
·1800	410·5	410·3	·520908	28·25	28·24
·1825	391·5	391·5	·546074	25·54	25·55
·1854	370·9	371·3	·579066	22·55	22·57
·1935	322·76	322·89	·643847	18·02	18·08
·198979	295·65	295·82	·670785	16·54	16·60
·217402	226·91	226·96	·810	11·11	11·24
·226909	200·90	200·96	·940	8·14	8·29
·235923	180·43	180·44	1·170	5·18	5·32
·241331	169·68	169·70	1·342	3·89	4·03
·262830	135·66	135·62	2·500	0·98	1·15
·273955	122·12	122·06	3·210	0·52	0·70

While the previous formulæ, with the single exception of Radhakrishnan's fail in the remote ultra-violet, this one fits very well from 6000 A.U. to 1525 A.U. In fact from 5800 A.U. to 1800 A.U., the maximum error is only about one part in a thousand, being sometimes positive, sometimes negative. Between 1800 A.U. and 1525 A.U., the deviation is slightly larger for certain wavelengths, but even so it is not of a progressive nature. There is a small discrepancy as we proceed from the red end of the spectrum to the infra-red, the error uniformly increasing with increase of wave-length. This is no doubt due to the contribution of the infra-red absorption bands, which have not been included in the above formula. As a matter of fact, Gutowsky (*loc. cit.*) has found that quartz exhibits anomalous rotary dispersion beyond 3·7 μ, the rotation, instead of decreasing as is to be expected,

increasing nearly four times from $3{\cdot}7\,\mu$ to $9{\cdot}7\,\mu$, thereby indicating that the presence of absorption bands in the infra-red has an influence on the optical rotatory power.

It can easily be shown that the single characteristic frequency used in the above rotary dispersion formula lies within the region of the ultra-violet spectrum in which the absorption frequencies of quartz appear. A one-term dispersion formula for the ordinary refractive index has been fitted up using this same frequency. The formula proposed is of the Sellmeyer-Drude type which is known to yield satisfactory results in the case of quartz (Radhakrishnan, 1951). The formula is

$$n_w^2 - 1 = \frac{1{\cdot}35\,\lambda^2}{\lambda^2 - (0{\cdot}0926283)^2}. \tag{7}$$

The calculated values are given in Table III.

TABLE III

Dispersion of quartz (for explanation see text)

λ (in μ)	n (experimental)	n (calculated)
·1854	1·676	1·673
·2413	1·605	1·607
·3404	1·5675	1·5678
·5086	1·548	1·548
·6708	1·541	1·541
·8000	1·538	1·539
1·2000	1·532	1·536

We see that the error in the calculated value over the whole range is only in the third decimal place. This indicates that the characteristic wave-length of 926 A.U. is roughly the same as the effective average wave-length of the absorption spectrum of quartz in the ultra-violet.

4. THE TEMPERATURE VARIATION OF THE OPTICAL ROTATORY POWER

The rotary dispersion formula (6) may be expressed in the form

$$\rho = \frac{a\nu^2}{(\nu_0^2 - \nu^2)^2}, \tag{8}$$

where 'a' is a constant such that $k = a\lambda_0^4$ and ν_0 is the characteristic absorption expressed in wave-numbers. The optical rotatory power of quartz is known to increase with rise of temperature even when the expansion

along the optic axis has been corrected for. To calculate this increment let us differentiate equation (8) with respect to temperature. We shall simply consider 'a' to be constant with temperature, but ν_0 to vary with it, so that

$$\frac{d\rho}{dt} = \frac{4a\nu^2\nu_0^2}{(\nu_0^2 - \nu^2)^3}\chi_0, \tag{9}$$

where

$$\chi_0 = -\frac{1}{\nu_0}\frac{d\nu_0}{dt} = \frac{1}{\lambda_0}\frac{d\lambda_0}{dt}.$$

Hence the temperature coefficient of the optical rotatory power

$$\frac{1}{\rho}\frac{d\rho}{dt} = \frac{4\lambda^2}{(\lambda^2 - \lambda_0^2)}\chi_0. \tag{10}$$

Molby (1910) has made precision measurements of the optical rotatory power of quartz at temperatures of $-118°$ C. and $20°$ C. from 4000 A.U. to 6700 A.U. With the aid of equation (9) and the rotatory dispersion formula (6), the values of $d\rho/dt$ have been theoretically accounted for over the whole range of wave-lengths. The value of χ used is $2{\cdot}7 \times 10^{-5}$. The theoretical values are given in Table IV.

TABLE IV

Temperature variation of optical rotatory power

λ (in μ)	ρ (experimental)		$\frac{d\rho}{dt}$ (expt.)	$\frac{d\rho}{dt}$ (theor.) $\chi = 2{\cdot}7 \times 10^{-5}$
	20° C.	−188° C.		
·4047	48·842	47·675	$5{\cdot}6 \times 10^{-3}$	$5{\cdot}6 \times 10^{-3}$
·4359	41·441	40·469	$4{\cdot}7 \times 10^{-3}$	$4{\cdot}7 \times 10^{-3}$
·4670	35·529	34·696	$4{\cdot}0 \times 10^{-3}$	$4{\cdot}0 \times 10^{-3}$
·4800	33·593	32·818	$3{\cdot}7 \times 10^{-3}$	$3{\cdot}8 \times 10^{-3}$
·5086	29·656	28·983	$3{\cdot}2 \times 10^{-3}$	$3{\cdot}3 \times 10^{-3}$
·5461	25·472	24·885	$2{\cdot}8 \times 10^{-3}$	$2{\cdot}8 \times 10^{-3}$
·5893	21·686	21·188	$2{\cdot}4 \times 10^{-3}$	$2{\cdot}4 \times 10^{-3}$
·6438	18·003	17·603	$1{\cdot}9 \times 10^{-3}$	$2{\cdot}0 \times 10^{-3}$
·6708	16·493	16·145	$1{\cdot}7 \times 10^{-3}$	$1{\cdot}8 \times 10^{-3}$

The agreement between the theoretical and experimental values is satisfactory. From equation (10) we notice that the theory predicts that the temperature coefficient of the rotatory power should exhibit an increase with decrease of wave-lengths. This in fact is known to be true from Molby's measurements and also from the observations of Soret and Sarasin (1882).

Le Chatelier (1889) has made measurements of the rotatory power over wide ranges of temperatures both below and above the α-β transformation

point in quartz. Using a value of $\chi = 4{\cdot}5 \times 10^{-5}$, dp/dt has been theoretically calculated as before. These are given in Table V.

TABLE V

Temperature variation of optical rotatory power

λ (in μ)	$\frac{d\rho}{dt}$ (experimental)	$\frac{d\rho}{dt}$ (theor.) $\chi = 4{\cdot}5 \times 10^{-5}$
·279	$27{\cdot}5 \times 10^{-3}$ (20° – 475° C.)	24×10^{-3}
·448	$7{\cdot}0 \times 10^{-3}$ (20° – 415° C.)	$7{\cdot}3 \times 10^{-3}$
·500	$5{\cdot}4 \times 10^{-3}$ (,,)	$5{\cdot}7 \times 10^{-3}$
·518	$5{\cdot}0 \times 10^{-3}$ (,,)	$5{\cdot}3 \times 10^{-3}$
·589	$4{\cdot}3 \times 10^{-3}$ (,,)	$4{\cdot}0 \times 10^{-3}$
·656	$3{\cdot}4 \times 10^{-3}$ (,,)	$3{\cdot}2 \times 10^{-3}$

The value of χ in this case has increased as the temperature is higher. In fact, as will be seen later, χ is found to have almost the same value and increase in roughly the same proportion with temperature, from the refraction data as well. Thus the increase of temperature coefficient with increase of temperature and with decrease of wave-length have both become intelligible from these calculations.

5. RELATION TO ORDINARY DISPERSION AND ITS THERMAL VARIATION

It would be of interest to see how the results obtained in the previous section are related to ordinary dispersion and its variation with temperature. Dispersion formulæ for quartz have been suggested by many authors in the past. We shall consider here only that put forward by Radhakrishnan (*loc. cit.*) which has the merit of fitting both the ordinary and extraordinary indices very accurately. We shall quote only that for the ordinary index, *viz.*,

$$n_\omega^2 - 1 = \frac{0{\cdot}663044\,\lambda^2}{\lambda^2 - (0{\cdot}0600)^2} + \frac{0{\cdot}517852\,\lambda^2}{\lambda^2 - (0{\cdot}1060)^2} + \frac{0{\cdot}175912\,\lambda^2}{\lambda^2 - (0{\cdot}1190)^2} + \frac{0{\cdot}565380\,\lambda^2}{\lambda^2 - (8{\cdot}844)^2} + \frac{1{\cdot}675299\,\lambda^2}{\lambda^2 - (20{\cdot}742)^2}. \qquad (11)$$

In this formula, the absorption at 600 A.U. is a hypothetical one, while those at 1060 A.U. and 1190 A.U. correspond with the reflection maxima observed by Tousey (*loc. cit.*). In addition, there are two small infra-red terms which serve to give a very accurate fit over the entire range of available data.

It is quite possible, of course, that the characteristic wave-length at 926 A.U. which determines the optical rotatory power also plays a sensible role in the ordinary dispersion of quartz. Accordingly, a dispersion formula for the ordinary index of quartz has been fitted up in which this wave-length has been included. The absorptions at 600, 1060 and 1190 A.U. have been retained, but an additional one at 926 A.U. has been introduced. The formula is

$$n_w^2 - 1 = \frac{0{\cdot}6504\,\lambda^2}{\lambda^2 - (0{\cdot}0600)^2} + \frac{0{\cdot}1000\,\lambda^2}{\lambda^2 - (0{\cdot}0926283)^2} + \frac{0{\cdot}384\,\lambda^2}{\lambda^2 - (0{\cdot}1060)^2} + \frac{0{\cdot}2228\,\lambda^2}{\lambda^2 - (0{\cdot}1190)^2} - 0{\cdot}01193\,\lambda^2. \qquad (12)$$

The agreement between the calculated and the experimental values can be seen in Table VI below.

TABLE VI

Dispersion of quartz (for explanation see text)

λ (in μ)	n_w (expt.)	n_w (calc.)
·185467	1·67578	1·67578
·214439	1·63039	1·63038
·291358	1·58098	1·58096
·340365	1·56747	1·56747
·479991	1·55012	1·55012
·58929	1·54425	1·54425
·670786	1·54147	1·54146

The accuracy of this formula is seen to be as good as any of the formulæ suggested previously.

Measurements of dn/dt have been made by Radhakrishnan (*loc. cit.*) over a wide range of temperatures for several wave-lengths. Using the data for the ordinary index, the χ's for the several dispersion frequencies occurring in Formulæ (11) and (12) have been calculated in the manner suggested by Ramachandran (1947). Since the contribution of the infra-red frequencies is small, their variations with temperature have been neglected. It is found that the data agree well when it is assumed that the extreme ultra-violet term at 600 A.U. is unaffected by temperature in both the formulæ. In Formula (11) we shall assume that the χ's for 1060 A.U. and 1190 A.U. are the same, as these two terms are very close to each other. Similarly,

in Formula (12) we shall assume that the χ's for 926, 1060 and 1190 are the same. The χ's calculated from the two formulæ are tabulated below.

TABLE VII

Temperature variation of refractive index

λ (in μ)	Temperature 50° C.			Temperature 400° C.		
	$-\frac{dn}{dt}\times 10^5$ (expt.)	$\chi\times 10^5$ Formula (11)	$\chi\times 10^5$ Formula (12)	$-\frac{dn}{dt}\times 10^5$ (expt.)	$\chi\times 10^5$ Formula (11)	$\chi\times 10^5$ Formula (12)
·2537	0·29	2·3	2·3	1·00	3·5	3·4
·3650	0·54	2·2	2·1	1·32	3·3	3·3
·5461	0·62	2·1	2·1	1·44	3·3	3·2
·5893	0·63	2·1	2·1	1·46	3·2	3·2

It will be noticed that the values of χ obtained from formulæ (11) and (12) are almost the same. It will also be seen on comparing the above table with Tables IV and V that the χ's estimated from the data on the thermal variation of refraction and the thermal variation of rotation are about the same and also increase in the same manner with rise of temperature.

6. DISCUSSION

The fact that the rotary dispersion of quartz is expressible by a formula of the type

$$\rho = \frac{k\lambda^2}{(\lambda^2-\lambda_0^2)^2}$$

indicates that its optical activity is a result of an interaction or coupling between the successive polarisable units in the structure of the crystal excited to similar upper energy levels, or in other words, an interaction in the nature of resonance. In their article in the *Handbuch der Physik*, Born and Goppert-Mayer (1933) arrive at the general formula

$$\rho = \sum_r \frac{P_r\lambda^2}{(\lambda^2-\lambda_r^2)^2} + \frac{Q_r}{\lambda^2-\lambda_r^2} + \sum_v \frac{P_v\lambda^2}{(\lambda^2-\lambda_v^2)^2} + \frac{Q_v}{\lambda^2-\lambda_v^2}.$$

It will be noticed in this formula, that in addition to terms of the Drude type, certain quadratic terms, of the same form as suggested in this paper, are also present. In view of the close agreement between the experimental values and the values calculated from the author's formula (see Table II), it appears improbable that terms of the Drude type play any observable role

in determining the optical rotatory power of quartz in the region of the visible and the ultra-violet part of the spectrum.

In conclusion, I express my sincere gratitude to Prof. Sir C. V. Raman, F.R.S., N.L., for the kind advice and the encouragement he gave me during the course of this investigation.

7. Summary

Numerous formulæ have been proposed by several authors to account for the rapid increase in the rotatory power of quartz with decrease of wavelength. These formulæ generally consist of a large number of terms both positive and negative, principally of the Drude type, involving various hypothetical characteristic frequencies. An examination of these formulæ shows that they do not possess physical justification and are arbitrary in character. In the present investigation it is shown that the data are well represented by the single term formula

$$\rho = \frac{k\lambda^2}{(\lambda^2-\lambda_0^2)^2} \text{ or } \frac{a\nu^2}{(\nu_0^2-\nu^2)^2},$$

where $k = 7{\cdot}186$ and $\lambda_0 = 0{\cdot}0926283\,\mu$. Assuming that '$a$' is a constant with temperature and ν_0 to vary with it, the thermal variation of the optical rotatory power has been quantitatively accounted for, ν_0 being found to vary in the same manner with temperature as estimated from the thermal variation of the refractive indices of quartz.

References

Born and Goppert-Mayer	..	*Hand. der Phys.*, 1933, **24/2**, 664.
Bradshaw and Livens	..	*Proc. Roy. Soc.*, 1929, **122**, 245.
Duclaux and Jeantet	..	*Journ. de Phys.*, 1926, **7**, 200.
Gutowsky	..	*Journ. Chem. Phys.*, 1951, **19**, 438.
Le Chatelier	..	*Comp. Rend.*, 1889, **109**, 264.
	..	*Bull. Soc. Franc. Min.*, 1890, **23**, 119.
Lowry	..	*Phil. Trans.*, 1912, **212 A**, 261.
	..	*Optical Rotatory Power*, 1935.
Molby	..	*Phys. Rev.*, 1910, **31**, 291.
Radhakrishnan	..	*Proc. Ind. Acad. Sci.*, 1947, **25**, 260.
	..	*Ibid.*, 1951, **33**, 22.
Ramachandran	..	*Ibid.*, 1947, **25**, 266.
Servant	..	*Comp. Rend.*, 1938, **207**, 283.
Soret and Sarasin	..	*Arch. Sc. Phys. Nat.*, 1882, **8**, 5; 1882, **8**, 97; 1882, **8**, 201.
Sosman	..	*Properties of Silica*, 1927.
Tousey	..	*Phys. Rev.*, 1940, **57**, 1060.

INTERACTION OF THIONYL CHLORIDE AND ESTERS OF AROMATIC HYDROXY ACIDS AND THEIR DERIVATIVES IN PRESENCE OF FINELY DIVIDED COPPER—IV

Interaction of Methyl-β-Resorcylate and Thionyl Chloride in Presence of Finely Divided Copper

BY G. V. JADHAV AND V. N. DESHPANDE

(Karnatak College, Dharwar, and Organic Chemistry Laboratory, The Institute of Science, Bombay)

Received November 10, 1951

(Communicated by Dr. Mata Prasad, F.A.SC.)

IT was observed by Hirwe, Jadhav and Chakradev[1] that the reaction of thionyl chloride and methyl β-resorcylate in presence of finely divided copper was very vigorous and no definite product could be isolated. It has, however, been now found that diaryl disulphide (dithio-ether) could be isolated when the reaction was carried out at a lower temperature.

The point of linking of the two nuclei in this disulphide was arrived at by treating it with nitric acid in presence of sulphuric acid below −5° when 5-nitro-β-resorcylic acid was obtained, which showed that the two nuclei were linked through sulphur atom which occupied the position para to −OH group and meta to $-COOCH_3$ group. If, however, this nitric acid reaction was carried out at room temperature 3:5-dinitro-β-resorcylic acid was obtained.

The disulphide should have the constitution as $\begin{matrix} R \\ R \end{matrix}\!\!>\!S = S$ (where R is the nucleus) and not R—S—S—R as it gave 2:2′-dimethoxy-4:4′-dihydroxy-5:5′-dicarbmethoxy-diphenyl thioether when methylated with dimethyl sulphate in presence of alkali. This thioether gave 2:2′-dimethoxy-4:4′-dihydroxy-5:5′-dicarboxy-diphenyl thioether identical with the one got by Hirwe, Jadhav and Chakradev (*loc. cit.*). If the thioether would be supposed to have the constitution R—S—S—R both sulphur atoms should have been lost simultaneously.

As the same disulphide (dithioether) was formed by the action of sulphur monochloride as well as that of sulphur dichloride, the mechanism of the reaction may be explained by considering that thionyl chloride first decomposes as (1)[2] or (2)

$$3\,Cu + 4\,SOCl_2 \rightarrow 3\,CuCl_2 + 2\,SO_2 + S_2Cl_2 \qquad (1)$$

$$Cu + 2\,SOCl_2 \rightarrow CuCl_2 + SO_2 + SCl_2 \qquad (2)$$

and then $2\,SCl_2 \rightarrow S_2Cl_2 + Cl_2$.

As the yield of the disulphide with sulphur dichloride and sulphur monochloride is poor as compared with that obtained with thionyl chloride and copper, copper may be acting as catalyst also in this reaction. Further as the yield with sulphur dichloride is better than with monochloride, chlorine formed by its decomposition may be acting as a catalyst.

Sulphur monochloride has been known to form dithioethers (disulphide) by Naik[3] and Naik and Bhat.[4]

The diacetyl and dibenzoyl derivatives of the disulphide were also prepared.

Experimental

2:2′-4: 4′-*Tetrahydroxy*-5: 5′-*dicarbmethoxy-diphenyl disulphide* (*I*).—Methyl-β-resorcylate (6 g.) and thionyl chloride (25 c.c.) were mixed together and the mixture was surrounded by ice. Finely divided copper (8 g.) was gradually added to it. Fumes of hydrogen chloride and sulphur dioxide were evolved. The reaction mixture was protected from moisture and kept overnight in refrigerator. It was then mixed with dry chloroform and heated on a boiling water-bath for two hours and the hot solution filtered. A pasty mass was obtained after the removal of the liquid, which turned into solid after repeated washings with acetone. The solid was then boiled with carbon disulphide to remove free sulphur and finally crystallised from a mixture of nitrobenzene and acetic acid, m.p. 245–6°. Yield: 4 g. Found: S, 16·1; $C_{16}H_{14}O_8S_2$ requires S, 16·08 per cent.

5-*Nitro-β-resorcylic acid.*—The disulphide (I) (0·5 g.) was dissolved in sulphuric acid (5 c.c.) and the solution was surrounded by freezing mixture. Nitric acid (con.) (5 c.c.) was gradually added to it, not allowing the temperature to rise above −5°. The reaction mixture was kept in ice after the addition was over and then diluted with water when solid was obtained, which crystallised from hot water. m.p. 215–6°. This showed no lowering in melting point when mixed with a genuine specimen.

3:5-*Dinitro-β-resorcylic acid.*—The disulphide (I) was dissolved in sulphuric acid (5 c.c.) and nitric acid (con.) (5 c.c.) was added to it when a vigorous reaction commenced which was allowed to proceed for ten minutes. The precipitate obtained on diluting the mixture with water was crystallised from dilute acetic acid. It sintered at 190° and melted completely at 204° (decomposition). It showed no lowering in melting point when mixed with a genuine specimen.

2: 2′-*Diacetoxy*-4: 4′-*dihydroxy*-5: 5′-*dicarbmethoxy-diphenyl disulphide* (*II*).—It was prepared by acetylating (I) in presence of pyridine. Crystallised from glacial acetic acid, m.p. 213–4° (decomposition). Found: S, 13·4; $C_{20}H_{18}O_{10}S_2$ requires S, 13·3 per cent.

2:2′-*Dibenzoyloxy*-4:4′-*dihydroxy*-5:5′-*dicarbmethoxy-diphenyl disulphide* (*III*).—It was crystallised from acetic acid. It shrinks at 170° and melts at 191–2° (decomposition). Found: S, 10·3; $C_{30}H_{22}O_{10}S_2$ requires S, 10·6 per cent.

2:2′-*Dimethoxy*-4 : 4′-*dihydroxy*-5 : 5′-*dicarbmethoxy-diphenyl sulphide* (*IV*).—This was obtained when the disulphide (I) (0·5 g.) was heated on a boiling water-bath with dimethyl sulphate (5 c.c.) in presence of 20% solution of potassium hydroxide (40 c.c.). It crystallised from acetic acid in colourless needles which did not melt upto 300°. Found: S, 7·7; $C_{18}H_{18}O_8S$ requires S, 8·1 per cent.

This sulphide (IV) was hydrolysed to 2:2′-dimethoxy-4:4′-dihydroxy-5:5′-dicarboxy-diphenyl sulphide by boiling it for 2 hours with 10 per cent. sodium hydroxide solution. It crystallised from acetic acid, m.p. 224–5°. Found: S, 8·6; $C_{16}H_{14}O_8S$ requires S, 8·7 per cent. Hirwe, Jadhav and Chakradev (*loc. cit.*) gave m.p. 226°.

It showed no lowering in melting point when mixed with the genuine specimen.

The same disulphide (I) was also prepared by allowing sulphur dichloride (5 c.c.) to interact with methyl β-resorcylate (4 g.) in presence of dry ether (20 c.c.) and allowing the reaction to proceed for two days at room temperature. The semi-solid obtained after the removal of ether was stirred with carbon disulphide when grey solid separated. It crystallised from acetic acid, m.p. 245–6°. Yield, 1·7 g. Found: S, 16·03; $C_{16}H_{14}O_8S_2$ requires S, 16·08 per cent.

Sulphur monochloride also gave the same product when the reaction was allowed to proceed at room temperature for two days, but the yield was very poor (0·7 g. only from 4 g. of ester).

SUMMARY

The disulphide was obtained in this reaction and it was found to be unstable towards alkali. Its characteristic derivatives such as di-acetoxy and di-benzoyloxy were prepared.

REFERENCES

1. Hirwe, Jadhav and Chakradev .. *J. Univ. Bom.*, 1933, **2** (2), 128–31.
2. Silberard .. *J. Soc. Chem. Indust.*, 1926, **45**, 36–38 ; 55–57.
3. Naik .. *Soc.*, 1921, 379 ; 1231.
4. ——— and Bhat .. *J. Ind. Chem. Soc.*, 1927, **4**, 525–30.

THE OPTICAL PROPERTIES OF TITANIUM DIOXIDE

By T. Radhakrishnan*

(From the Department of Physics, Indian Institute of Science, Bangalore)

Received December 20, 1951

(Communicated by Prof. R. S. Krishnan, F.A.SC.)

1. Introduction

Titanium dioxide exists in three polymorphic varieties, namely, rutile and anatase (tetragonal) and brookite (orthorhombic). These structures are alternative forms of 6:3 co-ordination. All the forms are strongly absorbing below the blue region, the absorption being usually enhanced by impurities. The refractive indices are of the order of 2·5 to 3·0, with correspondingly large values of dispersion and birefringence. Measurements of dispersion have been made by many workers chiefly Schröder (1928) whose data have been used in the International Critical Tables (Vol. VII) to furnish dispersion data and estimates of dn/dt. The principal thermal expansion coefficients of rutile and anatase have been measured by Fizeau (1866) and those of brookite by Schrauff (1884). These data on refraction and expansion have been used here to compute dispersion formulæ for the three forms and calculate the temperature shift of the ultra-violet dispersion frequencies. Finally, the refractive indices of rutile have been calculated by Bragg's method and good accord obtained with the observed values.

2. Dispersion Formulæ for Titanium Dioxide

Schröder's dispersion data (Schröder, *loc. cit.*) range from 4,500 to 7,000 Å and are sufficiently extensive to locate the nearest ultra-violet dispersion frequency and suggest a correction for infra-red effects. Thus the proposed formulæ are of the form

$$n^2 - 1 = a + \frac{b\lambda^2}{\lambda^2 - \lambda_0^2} - c\lambda^2. \qquad (1)$$

The value of λ_0 can be made the same in all the three modifications, namely, 0·2870 μ. The other constants of the dispersion formulæ and the agreement between calculated and observed indices are shown in the succeeding tables.

---

* Now Scientific Officer in ATIRA, Ahmedabad.

TABLE I

Dispersion Formulæ for Anatase

Index	a	b	c
ω	2·4485	2·3998	0·10
ϵ	2·8325	1·8492	0·18

λ (in μ)	n_ω (calc.)	n_ω (obs.)	n_ϵ (calc.)	n_ϵ (obs.)
0·43583	2·7688	2·7688	2·6576	2·6576
0·49161	2·6584	2·6579	2·5688	2·5679
0·54607	2·5948	2·5951	2·5161	2·5166
0·57907	2·5679	2·5683	2·4936	2·4939
0·60727	2·5498	2·5498	2·4793	2·4793
0·67163	2·5179	2·5179	2·4518	2·4507
0·70820	2·5072	2·5039	2·4404	..

TABLE II

Dispersion Formulæ for Rutile

Index	a	b	c
ω	2·2868	2·7275	0·10
ϵ	2·6034	3·7199	0·20

λ (in μ)	n_ω (calc.)	n_ω (obs.)	n_ϵ (calc.)	n_ϵ (obs.)
0·54607	2·6505	2·6505	2·9467	2·9467
0·57907	2·6211	2·6214	2·9085	2·9100
0·60727	2·6001	2·6003	2·8842	2·8842
0·67163	2·5643	2·5648	2·8397	2·8397
0·69075	2·5555	2·5555	2·8294	2·8294
0·70820	2·5495	2·5495		

TABLE III

Dispersion Formulæ for Brookite

Index	a	b	c
α ..	2·9858	2·1036	0·18
β ..	2·6957	2·3130	0·16
γ ..	2·4285	2·9641	0·05

λ (in μ)	n_α (calc.)	n_α (obs.)	n_β (calc.)	n_β (obs.)	n_γ (calc.)	n_γ (obs.)
0·43583	2·7686	2·7695	2·7838	2·7837	2·9419	2·9416
0·49161	2·6708	2·6717	2·6770	2·6769	2·8046	..
0·54607	2·6150	2·6154	2·6159	2·6160	2·7402	2·7402
0·57907	2·5910	2·5904	2·5895	2·5900	2·7094	2·7091
0·60727	2·5743	2·5739	2·5718	2·5718	2·6882	2·6882
0·67163	2·5441	2·5443	2·5405	2·5403	2·6518	2·6519
0·69075	2·5369	2·5375	2·5331	2·5328	2·6433	2·6429
0·70727	2·5312	2·5317	2·5279	2·5265	..	..

A perusal of these tables shows that the formulæ give results usually correct to the third decimal place, *i.e.*, within the limits of experimental error. The nearness and the large strength of the term at 2870 Å are responsible for the high refractive indices and dispersion. Since the constants a and b are approximately equal, the farther ultra-violet absorptions have together about the same strength in refraction as the nearest term. The infra-red correction term c has values of the order of 0·1 to 0·2, as compared with 0·1 in quartz. Since the Raman spectrum (Narayanan, 1950) of rutile and the absorption data of titanium dioxide do not indicate any near infra-red absorption, the infra-red vibrations must have very large strengths. This is supported by the exceptionally high dielectric constants (of the order of 50 to 100) of all the three forms at room temperature (Eucken and Buchner, 1934).

The near ultra-violet dispersion frequency is the same in rutile, anatase and brookite and hence the actual absorption peaks in this region must be nearly the same. This fact is understandable when we remember that in

all the three modifications, each oxygen has for its nearest neighbour three titanium atoms at the corners of a distorted equilateral triangle and each titanium atom has six oxygens as nearest neighbours at the corners of a distorted regular octahedron. The dispositions and distances of these atoms differ but little in the three forms (Bragg, *Atomic Structure of Minerals*, p. 104). Consequently the dispersion frequency is also nearly the same. It may be remarked that the situation in crystal and vitreous quartz is analogous. For both these, Tousey (1940) reports peaks of selective reflection in the same wavelength regions.

3. Thermo-Optic Behaviour of Titanium Dioxide

The thermo-optic coefficients dn/dt for the principal refractive indices of the three forms computed from Schröder's data are given in the International Critical Tables. The values are extremely rough and can be used only to make approximate calculations on the basis of the theory of thermo-optic behaviour for anisotropic crystals (Ramachandran, 1947).

Anatase.—In terms of Ramachandran's theory, we can form for a uniaxial crystal the functions

$$F_\omega = 2n_\omega \frac{dn_\omega}{dt} + \gamma_t (n_\omega^2 - 1) = A_\omega - \frac{\Delta P}{2(\nu_0^2 - \nu^2)} + \frac{2b_\omega \nu_0^4}{(\nu_0^2 - \nu^2)^2} \chi_t \quad (2)$$

$$F_\epsilon = 2n_\epsilon \frac{dn_\epsilon}{dt} + \gamma_t (n_\epsilon^2 - 1) = A_\epsilon + \frac{\Delta P}{\nu_0^2 - \nu^2} + \frac{2b_\epsilon \nu_0^4}{(\nu_0^2 - \nu^2)^2} \chi_t$$

where γ_t is the coefficient of volume expansion of the crystal at the temperature t, A_ω, A_ϵ are contributions to dn/dt from remote ultra-violet terms and ΔP represents a factor controlling the transfer of transition probability of the term at 2870 Å from axial to perpendicular directions as the temperature is increased. The last term gives the contribution to dn/dt from the temperature shift of the term with ν_0 at 2870 Å, the shift being defined by

$$\chi_t = -\frac{1}{\nu_0}\frac{d\nu_0}{dt} = \frac{1}{\lambda_0}\frac{d\lambda_0}{dt}. \quad (3)$$

From equation (2) one can eliminate ΔP and χ_t in turn, obtaining the results

$$F_\epsilon + 2F_\omega = A_\epsilon + 2A_\omega + \frac{2(b_\epsilon + 2b_\omega)\nu_0^4}{(\nu_0^2 - \nu^2)^2} \chi_t \quad 2(a)$$

$$F_\epsilon b_\omega - F_\omega b_\epsilon = A_\epsilon b_\omega - A_\omega b_\epsilon + \frac{1}{2}\frac{b_\epsilon + 2b_\omega}{(\nu_0^2 - \nu^2)} \Delta P. \quad 2(b)$$

On plotting the left-hand side of Eq. 2 (a) against $(\nu_0^2 - \nu^2)^{-2}$, one should obtain a straight line, the slope of which gives χ_t and the γ- intercept

$(A_\epsilon + 2A_\omega)$. Similarly from Eq. 2 (*b*) one can graphically estimate ΔP and $(A_\epsilon b_\omega - A_\omega b_\epsilon)$. A_ω and A_ϵ can also be separately evaluated. The points show considerable scatter in these graphs, but from the mean straight lines, one obtains the values

$$\Delta P = 120 \times 10^{-5}, \quad A_\omega = -5{\cdot}0 \times 10^{-5}, \quad A_\epsilon = -15{\cdot}0 \times 10^{-5},$$
$$\chi_t = 1{\cdot}23 \times 10^{-5}.$$

Using these constants, the calculated values of F_ω and F_ϵ are compared in Table IV with those directly obtained from *dn/dt* and γ. The value of γ was taken as $2{\cdot}18 \times 10^{-5}$ as obtained from Fizeau's data extrapolated to 90° C., the mean temperature of Schröder's observations.

TABLE IV

Thermo-Optic Coefficients of Anatase at 90° *C.*

λ (in μ)	$10^5 \cdot \frac{dn_\omega}{dt}$	$10^5 \cdot \frac{dn_\epsilon}{dt}$	$10^5 \cdot F_\omega$ (obs.)	$10^5 \cdot F_\omega$ (calc.)	$10^5 \cdot F_\epsilon$ (obs.)	$10^5 \cdot F_\epsilon$ (calc.)
0·4358	−1·8	+0·4	4·6	4·7	15·4	15·4
0·4916	−2·4	−0·6	0·5	1·1	9·1	8·9
0·5461	−2·5	−0·8	−0·5	−0·8	7·6	6·0
0·6073	−2·4	−1·3	−0·3	−1·3	4·8	4·1
0·6908	−2·6	−1·8	−2·5	−2·5	2·1	2·4

Table IV shows that the formulæ fit well the general trend of the observed values, but the casual errors in the latter are so large that a more accurate picture is not possible. It is for this reason that *dn/dt* has not been explicitly evaluated, the functions F_ω and F_ϵ being more suitable for comparison between theory and experiment since they are more smoothed out.

Brookite.—In this crystal, the refractive indices are very nearly the same and so too their temperature coefficients. One can therefore form the functions F_a, F_b, F_c and write

$$\left.\begin{aligned} \frac{(F_a + F_b)}{2} &= \tfrac{1}{2}(A_a + A_b) + \frac{\Delta P}{2(\nu_0^2 - \nu^2)} + \frac{(b_a + b_b)\nu_0^4 \chi_t}{(\nu_0^2 - \nu^2)^2} \\ F_c &= A_c - \frac{\Delta P}{\nu_0^2 - \nu^2} + \frac{2b_c \nu_0^4 \chi_t}{(\nu_0^2 - \nu^2)^2} \end{aligned}\right\} \quad (4)$$

Using the value $\gamma_{90} = 5{\cdot}57 \times 10^{-5}$ calculated from the observations of Schrauff, one obtains the coefficients

$$\tfrac{1}{2}(A_a + A_b) \approx 0; \quad A_\epsilon = 10 \times 10^{-5}; \quad \chi_t = 2{\cdot}47 \times 10^{-5}; \quad \Delta P = 440 \times 10^5$$

The calculated and observed values of $(F_a+F_b)/2$ and F_c are shown in Table V.

TABLE V

Thermo-Optic Coefficients of Brookite at 90° C.

λ (in μ)	$10^5.\frac{dn_a}{dt}$	$10^5.\frac{dn_b}{dt}$	$10^5.\frac{dn_c}{dt}$	$10^5.(F_a+F_b)/2$ calc.	$10^5.(F_a+F_b)/2$ obs.	$10^5.F_c$ (Cal.)	$10^5.F_c$ obs.
0·4358	5·1	5·3	..	66·3	66·3	..	..
0·4916	3·7	3·0	−8·4	52·9	52·3	−11·4	− 8·8
0·5461	2·4	2·1	−9·1	45·9	45·3	−12·2	−13·6
0·5790	2·4	1·9	−8·9	43·0	42·0	−12·4	−12·9
0·6708	2·0	1·4	−8·9	38·0	39·1	−14·5	−13·6
0·7082	1·7	1·3	..	37·3	37·7	..	..

As in the case of anatase, the calculated and experimental values have the same general trend. Owing to the large casual errors in the latter, a more accurate treatment is not possible. The values of χ_t and the transfer coefficient are twice the corresponding terms in anatase.

Rutile.—Schröder's measurements of $\frac{dn}{dt}$ in this crystal are confined to three wave-lengths, *viz.*, 5461, 5790 and 6234 Å. These three readings exhibit such large casual errors that they cannot be used for a computation of thermo-optic behaviour.

In general, neither the dispersion nor the thermo-optic behaviour of the three forms is known with sufficient accuracy to enable one to calculate the dispersion frequencies and their temperature shifts in a systematic manner. The data for anatase and brookite show, however, that the theory of thermo-optic behaviour for anisotropic crystals, which postulates a transfer of transition probability, as well as a temperature shift of the dispersion frequencies, can explain these cases. The transfer terms are found to be very large and contribute substantially towards the temperature variation of birefringence. On the other hand, the values of χ are comparatively small.

4. THE REFRACTIVE INDICES OF RUTILE

An absolute calculation of the birefringence of rutile and anatase has been made by Hylleraas (1926), based on Born's method (1918). We shall

perform this calculation in the case of rutile by the much simpler method of Bragg (1924), to see whether the very large refractive indices and birefringence are explained in terms of the influence of crystal structure on polarisability. The rutile structure is tetragonal with the basis $Ti\,(000;\ \frac{1}{2}\frac{1}{2}\frac{1}{2})$ and $O\,(\pm\,\omega\,\omega\,0;\ \frac{1}{2}+\omega,\ \frac{1}{2}-\omega,\ \frac{1}{2})$, with $\omega = 0{\cdot}31$, $a = 4{\cdot}58$ Å and $c = 3{\cdot}73$ Å. The structure can be pictured this way. The titanium atoms are at the corners and the body-centre of the tetragonal unit cell. To each *Ti* at the corners are attached two oxygen atoms at equal distances, along the direction of one of the basal diagonals. To the *Ti* at the body centre are attached two oxygen atoms at the same distances but in the direction of the other basal diagonal.

In our calculations, it is more convenient to choose for the co-ordinate the two basal diagonals as the XY axes and the c or tetrad axis as Z. The co-ordinates of the neighbours of an oxygen atom within a sphere of 5 Å are easily calculated. Their description is given in Table VI, with reference to the chosen atom as origin. It will be seen that there are 42 oxygen and 13 titanium atoms within the sphere.

TABLE VI

Neighbours of an Oxygen Atom in Rutile

Kind and No. of atoms	Co-ordinates			Distance from origin (Å)
2 Ti ..	$w-\frac{1}{2}$,	$w-\frac{1}{2}$,	$\frac{1}{2}$	1·92
1 Ti ..	w	w	0	2·07
1 O ..	$1-2w$	w	0	2·46
8 O ..	w	$\frac{1}{2}-w$	$\frac{1}{2}$	2·78
2 O ..	0	0	1	2·95
2 O ..	$2w-\frac{1}{2}$	$\frac{1}{2}$	0	3·46
2 Ti ..	w	$w-1$	0	3·56
2 Ti ..	w	w	1	3·61
2 O ..	$1-2w$	0	1	3·87
1 O ..	$2w$	0	0	4·00
4 O ..	$2w-\frac{1}{2}$	$\frac{1}{2}$	1	4·55
4 O ..	$\frac{1}{2}$	$\frac{1}{2}$	0	4·58
4 Ti ..	w	$w-1$	1	4·62
8 O ..	$w-\frac{1}{2}$	$1-w$	$\frac{1}{2}$	4·87
2 O ..	$2w$	0	1	4·97
8 O ..	w	$\frac{1}{2}-w$	$3/2$	5·01

From the mean index of the ordinary and extraordinary rays, one can calculate the molar refractivity of O^{--} in rutile as 6·2 assuming that of Ti^{4+} to be 0·6 (*cf.* Fajans and Joos, 1924). Since the refractivity of the titanium ion is very small, one may assume that it is polarised as if in an isotropic medium. The polarisability tensor of the oxygen atom can be evaluated

by finding the field acting on it in different directions caused by the 42 oxygen and 13 titanium neighbours. The calculations are considerably simplified because the cross-products xy, yz, zx vanish by virtue of the symmetry of the crystal. Thus there is no component of the internal field at right angles to the electric vector.

When the electric vector is parallel to the optic axis, the calculations are very straightforward. When it is perpendicular to the optic axis (say along Ox or Oy) the polarisabilities of the oxygen atoms in the layers o, $\pm c$, $\pm 2c$, etc., will be different from those of the atoms in the layers $\pm \frac{c}{2}, \pm \frac{3c}{2}, \ldots$. But these values of polarisability are exactly interchanged when the electric vector rotates through 90°, by virtue of the tetragonal symmetry. Thus the refractive index is isotropic for directions at right angles to the optic axis. It is sufficient to calculate the polarisability of either type of oxygen atom for both the x and y directions of the electric vector. The mean of these values will be equivalent to the mean polarisability of both types of atoms for either direction of the electric vector. Thus the calculations become considerably simplified.

Bearing these points in mind we can write for the refractive indices n_3 and n_1 (n_e and n_ω)

$$\frac{n_k^2-1}{n_k^2+2} = \frac{\rho}{M}[c_k R_0 + R_{Ti}] \tag{5}$$

where M is the molecular weight and ρ the density (4·22) of rutile while R_0 and R_{Ti} are the molar refractivities. The anisotropy factor c_k is given by Bragg's theory as

$$c_k = 1 + \frac{3}{4\pi N}\left[\sum_1^{42}\left(\frac{3\xi^2-r^2}{r^5}\right)_0 R_0 + \sum_1^{13}\left(\frac{3\xi^2-r^2}{r^5}\right)_{Ti} R_{Ti}\right] \tag{6}$$

where $\xi^2 = z^2$ or $(x^2+y^2)/2$ according as k is 3 or 1 and N is the Avogadro number. On calculating the summation in the right-hand side of (6), it turns out that $c_3 = 1{\cdot}030$ and $c_1 = 0{\cdot}965$.

Substituting these values in Eq. (5) the two refractive indices for the sodium line are found to be as shown below:

	Calculated	Observed
n_e	2·86	2·89
n_ω	2·61	2·62

The calculations show that these high indices and birefringence are caused by the large refractivity of the oxygen atom in rutile (nearly double

the value found in other crystals), as well as by a strongly anisotropic polarisability tensor (as in calcite) for instance.

Similar calculations made for anatase taking into account the influence of all neighbours within a sphere of radius 6 Å gave the correct sign for the birefringence, *i.e.*, $n_\varepsilon < n_\omega$, but the magnitude of the calculated birefringence was twice as large as the observed value. The author believes that more neighbours will have to be considered if the birefringence is to be determined accurately both in the case of anatase as well as of rutile, and the excellent agreement found with rutile is fortuitous.

I express here my thanks to Professor R. S. Krishnan for his kind interest in this work and to Dr. G. N. Ramachandran for suggestions and advice.

Summary

Dispersion formulæ valid in the visible region are offered for rutile, anatase and brookite. These incorporate a characteristic frequency at 2870 Å in all the cases. The value of dn/dt in the three crystals are explained by large transfers of transition probability and moderate shifts towards larger wave-lengths of this frequency as the temperature is raised. In addition, a calculation is made of the refractive indices and birefringence of rutile on the basis of Bragg's theory and the results are in good accord with the observed data.

References

1. Born .. *Ann. d. Phys.*, 1918, **55**, 177.
2. Bragg .. *Proc. Roy. Soc.*, 1924, **105 A**, 370; **106**, 346.
   ———— .. *Atomic Structure of Minerals*, 1937, 104.
3. Eucken and Buchner .. *Zeits. f. Phys. Chem.*, 1934, **27 B**, 321.
4. Fajans and Joos .. *Zeits. f. Phys.*, 1924, **23**.
5. Fizeau .. *Ann. d. Phys.*, 1866, **128**, 564.
6. Hylleraas .. *Zeits. f. Kryst.*, 1927, **44**, 871.
7. Narayanan .. *Proc. Ind. Acad. Sci.*, 1950 **A**, **32**, 279.
8. Ramachandran .. *Ibid.*, 1947, **26**, 77.
9. Schrauff .. *Zeit. f. Kryst.*, 1884, **9**, 433.
10. Tousey .. *Phys. Rev.*, 1940, **57**, 1060.

MAXWELL EFFECT IN SOME SIMPLE ORGANIC LIQUIDS: COMPARISON BETWEEN THEORY AND EXPERIMENT

By T. S. Narasimhamurty

(*From the Physical Laboratories, Osmania University, Hyderabad*)

Received December 20, 1951

(Communicated by Prof. S. Bhagavantam, F.A.SC.)

1. Introduction

The mechanical birefringence in liquids (Maxwell Effect) was extensively studied by Vörlander and Walter (1925). This led Raman and Krishnan (1928) to formulate a molecular theory for this phenomenon, in analogy with their theory explaining the electrical and magnetic birefringence of liquids. A quantitative comparison of the theoretical values with the experimental results was attempted by Paldhikar (1936) and Rao (1937) who showed that the calculated birefringence in the few cases verified by them was of the right order of magnitude. Since these papers were published, Buchheim, Stuart and Menz (1939) experimentally studied the Maxwell Effect in a few more simple organic liquids, thus providing a wider field for the verification of the theoretical ideas on the subject. An attempt is made now to critically examine these results in the light of Raman and Krishnan's theory.

2. Raman and Krishnan's Theory

Raman and Krishnan have shown from theoretical considerations, that the mechanical birefringence is a universal property which liquids may be expected to exhibit provided they are *both* geometrically and optically anisotropic. The Maxwell constant ∇ is shown to be equal to

$$\frac{(n^2-1)(n^2+2)}{10\,n\nu\mathrm{KT}} \cdot \frac{\Sigma\{(a-b)\}(\mathrm{A}-\mathrm{B})}{(\Sigma a)\times(\Sigma\,\mathrm{A})}, \qquad (1)$$

where n = refractive index of the liquid,

ν = number of molecules per unit volume,

K = Boltzmann Constant,

T = absolute temperature.

a, b, c are the principal geometrical dimensions of the molecules and A, B, C are their principal optical polarizabilities.

For a molecule possessing an axis of symmetry with $a = b$, equation (1) may be written thus;

$$\nabla = \pm \frac{(n^2-1)(n^2+2)}{10\,n\nu KT} \cdot \frac{2(c-a)}{2a+c} \sqrt{\delta}, \qquad (2)$$

where δ is the optical anisotropy.

3. Data and Calculations

Equation (2) may more conveniently be put down thus:

$$\nabla = \pm \frac{(n^2-1)(n^2+2)}{n} \cdot \frac{M}{10TRd} \cdot \frac{2(c-a)}{2a+c} \sqrt{\delta} \qquad (3)$$

The several constants given in Table I except a, c and δ for different liquids are obtained from International Critical Tables. The geometrical dimensions of the molecules, collected in Table I, are generally accepted values, arrived at from X-ray data and other evidence. Even though slight geometrical asymmetry in the plane is obvious in the case of some of the benzene ring molecules in Table I, it is not taken account of in putting down the dimensions, as this difference may be ignored in the first approximation.

The value of δ for the liquids [1-6] is taken from the existing literature wherever possible. For two liquids[7,8] it is calculated from a knowledge of β_T and ρ.

δ for mesitylene is not available from experiment and is therefore estimated by arguing that the structural change is progressive from benzene to toluene to *m*-Xylene to mesitylene. δ for toluene is $20{\cdot}4 \times 10^{-3}$, for *m*-Xylene it is $18{\cdot}8 \times 10^{-3}$ and hence it is reasonable to extrapolate and obtain δ for mesitylene as $17{\cdot}2 \times 10^{-3}$ (*i.e.*, the difference between the optical anisoptroy of *m*-xylene and that of mesitylene is assumed to be the same as that between that of toluene and of *m*-xylene). Evidence to this end is also forthcoming from the fact that as we go from benzene to toluene, the symmetrical structure of the ring is disturbed; but the symmetry is progressively reclaimed as we go from toluene to *m*-xylene and then to mesitylene. Thus mesitylene which is more symmetrical than *m*-xylene and toluene should have its δ in the vicinity of that of benzene.

δ for *o*-xylene is also not available from experiment and is estimated by arguing that the adiabatic compressibilities of the three xylenes are nearly the same (about 63×10^{-6}) and therefore, the isothermal compressibilities for the three xylenes should also be nearly the same. β_T for *p*-xylene is 92×10^{-6} and β_T for *m*-xylene is 91×10^{-6}. Hence it is reasonable to assume that β_T for *o*-xylene is 90×10^{-6}. The depolarization factor ρ for *o*-xylene is 40%. Using these values of β_T and ρ, δ is calculated in the usual manner.

The figures thus collected and the results of calculation, using formula (3), are shown in Table I. Experimentally observed values of the Maxwell Constant are compared with the corresponding calculated results.

TABLE I. *Maxwell Effect in Liquids*

Liquid	Molecular weight	Density	Refractive index	Temp.	Optical Anisotropy	Length of axes. A.U.		Maxwell constant calculated ∇	Maxwell constant experimental ∇	Reference for δ
	M	d	n	°C.	$\times 10^3$	a	c	$\times 10^{12}$	$\times 10^{12}$	
P-Xylene ..	106·1	0·861	1·496	20	38·5	7	3	164·0	275·2	(7)
Mesitylene ..	120·1	0·863	1·497	,,	17·2	9	3	122·8	196·1	..
M-Xylene ..	106·1	0·865	1·497	,,	18·8	7	3	115·5	193·2	(1)
Chlorobenzol ..	112·5	1·107	1·525	,,	30·6	7	3	130·4	186·1	(4)
O-Xylene .	106·1	0·879	1·506	,,	11·3	7	3	86·8	183·7	..
Toluol ..	92·06	0·866	1·496	,,	20·4	7	3	104·0	155·6	(2)
Benzene ..	78·05	0·878	1·501	,,	18·0	7	3	82·7	96·1	(3)
Heptyl alcohol ..	116·1	0·817	1·425	,,	2·2	4·6	11·34	52·37	58·43	(5)
Carbon tetrachloride	153·8	1·595	1·461	,,	1·6	a	a	a	<8·7	(6)
Cyclo-hexane ..	84·09	0·779	1·427	..	1·8	8	5	15·7	<4·3	(8)

4. DISCUSSION OF RESULTS

The following observations may be made in respect of results in Table I:

In all the liquids, there is a fair agreement between the theoretical and experimental values—in fact, the agreement is much better than that shown in the earlier work by Paldhikar (1936) and Rao (1937).

In all the cases, except cyclohexane, where the very low experimental value might not have been measured with reasonable accuracy, the theoretical value is less than the experimental value.

The ratio of the theoretical value to the experimental one in most cases is, surprisingly enough, almost the same, roughly $\frac{2}{3}$.

The larger experimental value cannot be attributed to turbulence or rise of temperature. Nevertheless, the main ideas underlying the theory appear to be correct.

In conclusion, the author desires to express his grateful thanks to Dr. S. Bhagavantam, Director, Physical Laboratories, Osmania University, Hyderabad, Deccan, for kindly suggesting the problem and for his keen interest and encouraging guidance in the course of the preparation of this paper.

REFERENCES

Vörlander, D. and Walter, R. .. *Z. Phys. Chem.*, 1925, **118**, 1.
Raman, C. V. and Krishnan, K. S. .. *Phil. Mag.*, 1928, **5**, 769.
Paldhikar .. *Ibid.*, 1936, **21**, 1125.
Rao, A. B. .. *Proc. Ind. Acad. Sci.* 1937, **5A**, 124.
Buchheim, W., Stuart, H. A. and Menz, H. *Zeits. f. Physik*, 1939, **112**, 7–8, 407–19.
——— .. *Science Abstracts*, 1939, **42**, Abs. 2890, p. 687.

ELASTIC PROPERTIES OF POLYCRYSTALLINE AGGREGATES

By S. Bhagavantam, F.A.Sc. and T. Seshagiri Rao

(From the Physical Laboratories, Osmania University, Hyderabad-Dn.)

Received April 17, 1951

1. Introduction

A polycrystalline aggregate will be elastically isotropic when the crystals that compose it are distributed uniformly over all directions, and in such a case, it will exhibit only two elastic constants which are independent of direction. Bridgman (1931 and 1932) determined the compressibilities of a number of cubic compounds by a static method. He worked with polycrystalline specimens obtained from dry powders after compression to about 310,000 lb./in.^{2} in a mould. Lawson (1940) also determined the compressibility, among other properties, of ammonium chloride using the composite piezoelectric oscillator method. He obtained the polycrystalline specimens from a block of material prepared by compressing dry granulated ammonium chloride to 50,000 lb./in.^{2} in a steel cylinder at room temperature.

The ultrasonic wedge method (1944) has been successfully used by us to study the elastic properties of single crystals during the past several years. It is now proposed to extend this method to a study of the elastic properties of polycrystalline aggregates. The present paper embodies the results of a preliminary investigation of some cubic compounds. There is a special advantage in this method, because it can be used for investigations at higher and lower temperatures without much difficulty and this will be attempted in our future work.

2. Mathematical Theory

The calculation of the properties of polycrystalline aggregates is based on the idea that the properties of the aggregates are average values of the properties of the individual crystals. The average value is obtained by summing up the values of the property of the crystals according to the frequency distribution of their orientations, and dividing this sum by the number of orientations employed. In the case of random orientation, the crystallographic axes are distributed with uniform frequency in all directions of space. Details of this process are given in a recent publication of Boas (1949).

In this way, the average value of C_{11}' can be obtained from the relation

$$(C_{11}')_{AV} = \frac{\int_{\theta=0}^{\pi}\int_{\phi=0}^{2\pi} C_{33}' \sin\theta \, d\theta \, d\phi}{\int_{0}^{\pi}\int_{0}^{2\pi} \sin\theta \, d\theta \, d\phi}$$

where $C_{33}' = (2C_{44} + C_{12}) + (C_{11} - C_{12} - 2C_{44})(\alpha_{13}^4 + \alpha_{23}^4 + \alpha_{33}^4)$ in the case of cubic system. α_{13}, α_{23} and α_{33} are the direction cosines and are given by

$$\alpha_{13} = \sin\theta\cos\phi, \quad \alpha_{23} = \sin\theta\sin\phi \text{ and } \alpha_{33} = \cos\theta.$$

Working out the integration, the expression for $(C_{11}')_{AV}$ comes out as

$$(C_{11}')_{AV} = \frac{3}{5} C_{11} + \frac{2}{5}(C_{12} + 2C_{44}).$$

The average value for C_{44}' can be obtained by performing the integration

$$(C_{44}')_{AV} = \int_0^{2\pi} \frac{d\psi}{2\pi} \int_0^{2\pi} \frac{d\phi}{2\pi} \int_0^{\pi} \frac{C_{44}' \sin\theta \, d\theta}{2},$$

where $C_{44}' = (\alpha_{12}^2 \alpha_{13}^2 + \alpha_{22}^2 \alpha_{23}^2 + \alpha_{32}^2 \alpha_{33}^2)(C_{11} - C_{12} - 2C_{44}) + C_{44}$ for cubic system.

α_{13}, α_{23} and α_{33} are the same as above and

$\alpha_{12} = -\cos\theta\cos\phi\sin\psi - \sin\phi\cos\psi$;

$\alpha_{22} = \cos\phi\cos\psi - \sin\phi\sin\psi\cos\theta$ and $\alpha_{32} = \sin\theta\sin\psi$.

Introducing these values and working out the integration, the expression for the average value for cubic crystals becomes

$$(C_{44}')_{AV} = \frac{3}{5} C_{44} + \frac{1}{5}(C_{11} - C_{12}).$$

These expressions have been derived also by Mason and McSkimin (1948 and 1949) in order to calculate the scattering factors for metals.

It may be noted that $(C_{11}')_{AV} - \frac{4}{3}(C_{44}')_{AV} = \frac{C_{11} + 2C_{12}}{3}$ which is the bulk modulus of the polycrystalline aggregate. This is not a third independent elastic constant. Further, if the crystal is such that the Cauchy relation $C_{12} = C_{44}$ holds good, the above equations become dependent on one another and reduce to

$$(C_{11}')_{AV} = 3(C_{44}')_{AV} = \frac{3}{5}(C_{11} + 2C_{12}).$$

From this, it follows that the bulk modulus K is given by the relation

$$K = \frac{5}{9}(C_{11}')_{AV} = \frac{5}{3}(C_{44}')_{AV}.$$

3. Experimental Technique

The experimental set-up used is essentially the same as that employed in the wedge method. Some of the alkali halides belonging to the cubic system, the elastic constants of which have been determined in the crystalline state, are chosen for the present investigation. Pure and dry substances are obtained, finely powdered and passed through a 200-mesh sieve. These powders are compressed in a steel mould between two high tensile steel cylinders of 1″ diameter. All the polycrystalline specimens in the present investigation are pressed at about 60,000 lb./in.^{2} The compressed cakes are then ground to uniform thickness on very fine emery cloth. Thus a uniformity of 1 to 2 in 100 is obtained. That the microcrystals composing the polycrystalline aggregate are oriented in a perfectly random manner as a result of such a compression has been tested by an X-ray study of one or two specimen tabloids.

The determination of the densities of these compressed cakes is a very important factor since the calculation of $(C_{11}')_{AV}$ and $(C_{44}')_{AV}$ involves a knowledge of the densities besides the appropriate characteristic frequencies. In all cases, the density is determined directly by evaluating the volume of the circular tabloid and determining its weight in air. In this way, densities of the various tabloids have been determined to an accuracy of 1 to 2 per cent.

It is shown by Walker (1923) that when a powder is pressed into a cylinder by a plunger, the density of the powder is not evenly distributed but is greatest immediately beneath the plunger, gradually falling off as the distance from the plunger increases. Attempts to detect such large variation in density have yielded negative results in the case of the present tabloids, because the maximum thickness does not exceed 3·5 mm. and in some cases, the thickness is only about 2 mm.

In the present investigation, while determining the characteristic frequencies of the tabloids, special care is taken to see that the tabloids do not come into direct contact with the liquid in the cell. Otherwise, the liquid gets into the pores of the specimens and vitiates the experimental results. For this purpose, the design of the crystal holder is slightly modified. The lower annular brass electrode on which the specimen under investigation rests, is now replaced by a brass cup-like vessel. The central hole of the latter is covered by a thin aluminium foil. The tabloid is placed on the aluminium foil with a drop of transformer oil in between for securing good

acoustical contact. The quartz wedge is kept on the top of the tabloid with another drop of transformer oil in between as usual. This oil, being dense, does not enter the pores of the tabloid as has been revealed by the constancy in the mass of the specimen just before and after the experiment, the weight being determined after wiping out the oil layer on the surface. But for this minor modification in the design of the crystal holder, the rest of the experimental set-up is just the same as that used for single crystals. The characteristic frequencies of the compressed specimens are determined in the usual way in the frequency range 2 to 10 Mc/Sec. The frequencies are measured using a precision heterodyne wavemeter capable of reading correct to within 1 in 50,000.

A feature to be mentioned here is that the power of the oscillator exciting the polycrystalline aggregate should neither be too great nor too low. If it is too great, a continuous diffraction pattern consisting of forced oscillations is observed instead of discrete maxima; if it is too low, no maxima will be observed due to the excessive absorption of the ultrasonic beam by the polycrystalline aggregate. Hence these two factors have to be reconciled and an optimum power just sufficient to give the discrete maxima should be used.

4. EXPERIMENTAL DATA AND RESULTS

The densities of the polycrystalline specimens pressed to about 60,000 lb./in.^{2}, determined by the method outlined in the previous section, are given in Table I along with the densities of the corresponding single crystals.

TABLE I

Densities of compressed tabloids

No.	Substance	ρ_{tabloid} g./cm.^{3}	ρ_{crystal} g./cm.^{3}
1	KCl ..	1·96	1·984
2	NaCl ..	2·12	2·168
3	NH_4Cl ..	1·50	1·527
4	KBr ..	2·67	2·756
5	KI ..	2·95	3·127

The average values $(C_{11}')_{AV}$ and $(C_{44}')_{AV}$ of the elastic constants calculated from the characteristic frequencies and the observed densities of the tabloids (column 3 in Table I), are given in units of 10^{11} dynes/cm.^{2} in Table II. The values of $(C_{11}')_{AV}$ and $(C_{44}')_{AV}$ calculated from the known single crystal constants using the expressions given in the second section, are compared with the measured results.

TABLE II

No.	Substance	Thickness in mm.	Fundamental frequency in Mc./Sec.	Mode of vibration	Effective elastic constant	Value	
						Measured	Calculated
1	KCl ..	2·29	0·866	l*	$(C_{11}')_{Av}$	3·08	3·18
	do ..	do	0·501	t*	$(C_{44}')_{Av}$	1·03	1·05
2	NaCl ..	3·24	0·705	l	$(C_{11}')_{Av}$	4·42	4·51
	do ..	do	0·407	t	$(C_{44}')_{Av}$	1·47	1·50
3	NH_4Cl ..	2·89	0·785	l	$(C_{11}')_{Av}$	3·09	3·17
	do ..	do	0·448	t	$(C_{44}')_{Av}$	1·01	1·04
4	KBr ..	3·00	0·503	l	$(C_{11}')_{Av}$	2·43	2·73
	do ..	do	0·290	t	$(C_{44}')_{Av}$	0·81	0·92
5	KI ..	1·83	0·644	l	$(C_{11}')_{Av}$	1·64	2·11
	do ..	do	0·378	t	$(C_{44}')_{Av}$	0·57	0·70

* Here, l and t denote the longitudinal and transverse modes respectively.

The values of the bulk modulus K calculated from the above experimental results using the relation $K = \frac{5}{9}(C_{11}')_{Av}$ are compared in Table III with those measured by direct experiment, in units of 10^{11} dynes/cm.^{2}

TABLE III

Sabstance	$(C_{11}')_{Av}$	$(C_{44}')_{Av}$	$K = {}^5/_9 (C_{11}')_{Av}$	K (direct measurement)
KCl ..	3·08	1·03	1·71	1·77
NaCl ..	4·42	1·47	2·46	2·40
NH_4Cl ..	3·09	1·01	1·72	1·79
KBr ..	2·43	0·81	1·35	1·50
KI ..	1·64	0·57	0·91	1·17

The experimental data concerning ammonium chloride and magnesium oxide available in the literature are given in Table IV.

TABLE IV

Substance	$\rho_{crystal}$	$\rho_{tabloid}$	K	Observer
NH_4Cl ..	1·527	..	1·77	Sundara Rao and Balakrishnan
	..	..	1·79	Bridgman
	..	1·520	1·77	Lawson
	..	1·512	1·66	do
MgO ..	3·57	..	16·6	Bridgman
	..	3·01	9·9	do

5. DISCUSSION OF RESULTS

Table I shows that the densities of the polycrystalline specimens approach the corresponding single crystal densities to within about 2 per cent. only in the case of the first three substances, *viz.*, potassium chloride, sodium chloride and ammonium chloride. The tabloid densities for the bromide and iodide of potassium are lower than the corresponding crystal densities by more than 3 per cent. and 6 per cent. respectively. These results show conclusively that all substances cannot be compressed to the same extent by the application of the same pressure. Similar conclusions were reached by Hagen (1919) who showed that it is not possible to compress quartz and barium sulphate to cohesive tablets while the alkali and other halides give very cohesive products. Further, the fact that the density of the pressed specimen of magnesium oxide with which Bridgman (1932) worked was only 3·01 in spite of the large pressure employed by him while the crystal density is 3·57, also shows that this substance is even worse than potassium iodide from this point of view.

Table II shows that in the case of the first three substances, whose densities lie within 2 per cent. of the crystal density, the measured average values of C_{11}' and C_{44}' are also lower than those calculated from the known single crystal constants by only about 2 to 3 per cent. In such cases, we may extrapolate the density and obtain the ideal elastic constant if required. On the other hand, in the case of potassium bromide and iodide where the densities of the specimens are lower than the crystal densities by more than 3 per cent. the deviations in the average values of elastic constants are disproportionately larger. In other words, the compressibility of a pressed specimen increases rapidly and out of proportion to the decrease in density, if we depart appreciably from the ideal densities. These results are in agreement with the observations of Bridgman in the case of magnesium oxide (Table IV) where a 18 per cent. fall of density is followed by a 40 per cent. fall in the bulk modulus. In our work, a 6 per cent. fall of density in the case of potassium iodide is followed by a 25 per cent. fall in the bulk modulus. On the other hand, Bridgman (1931) has also determined the compressibilities of a number of cubic substances like NH_4Cl, NaCl, KCl, KBr, etc., pressed at about 310,000 lb./in.^{2} and his values of compressibility agree well with those for single crystals available in the literature. But, as Lawson remarked, the densities of these specimens had not been reported by Bridgman and we have to presume that they are very close to the respective single crystal values.

In the case of ammonium chloride, Lawson however observed, as the figures in Table IV reveal, that the isothermal compressibility of a specimen

whose density is 1·512 gm./cm.^{3} is 6·7 per cent. greater than that of a specimen whose density is 1·520 gm./cm.^{3} It may be seen from the data that Lawson's value for the bulk modulus for a specimen of density 1·520 gm./cm.^{3} is slightly less than the value obtained by Bridgman. The latter author, however, did not give the density of the specimens with which he worked. Sundara Rao and Balakrishnan (1948) determined the elastic constants of single crystals of ammonium chloride. Their values lead to a bulk modulus of $1{\cdot}77 \times 10^{11}$ dynes per cm.^{2} which is in good agreement with the isothermal value of Lawson. However, Lawson's experimental result, that the lowering of density by 1 per cent. causes a fall of 6·7 per cent. in the bulk modulus does not fit in with the results of the present investigation; nor is it in agreement with the experimental results of Bridgman in the case of magnesium oxide.

The bulk moduli calculated from the values of $(C_{11}')_{AV}$ are compared in Table III with the standard values available in the literature. For the first three substances in which the densities approach the ideal values to within about 2 per cent., the moduli also approach the single crystal values to within about the same percentage.

6. Summary

The ultrasonic wedge method has been used for a determination of the average values $(C_{11}')_{AV}$ and $(C_{44}')_{AV}$ in the case of certain polycrystalline aggregates of cubic compounds prepared by compressing finely divided powder under high pressures. The measured values are compared with the values calculated from the known single crystal constants. It is found that certain substances can be compressed till their densities closely reach the single crystal densities and in those substances the average elastic properties also closely reach the corresponding ideal values. In other cases, the compressibility of a pressed specimen depends to a marked degree upon its density.

References

Bhagavantam, S. and Bhimasenachar, J. .. *Proc. Ind. Acad. Sci.*, 1944, **20**, 298.
Boas, W. .. *An Introduction to the Physics of Metals and Alloys*, 1949, p. 94.
Bridgman, P. W. .. *Phys. Rev.*, 1931, **38**, 182.
——— .. *Proc. Am. Acad. Sci.*, 1932, **67**, 345.
Hagen, T. V. .. *Zeits. Elektrochem.*, 1919, **25**, 375.
Lawson, A. W. .. *Phys. Rev.*, 1940, **57**, 417.
Mason, W. P. and McSkimin, H. J. .. *J. App. Phys.*, 1948, **19**, 940.
——— .. *Ibid.*, 1949, **20**, 228.
Sundara Rao, R. V. G. and Balakrishnan, T. S. *Proc. Ind. Acad. Sci.*, 1948, **28**, 480.
Walker, E. E. .. *Trans. Faraday Soc.*, 1923, **19**, 83.

A SIMPLE METHOD FOR THE STUDY OF VARIATION OF BOUNDARY TENSION WITH TIME

By R. S. Subrahmanya,* M. R. A. Rao and B. Sanjiva Rao, F.A.Sc.

Received September 21, 1951

Introduction

Several methods have been described in literature to measure the variation of boundary tension with time. Adam[1] has employed the maximum bubble pressure method to study the variation of surface tension with time, for a period of ten minutes, but concludes that the method is not suitable. Venkatachala[2] and Krishnappa[3] arrive at the same conclusion after employing this method to study the ageing of surfaces of aqueous solutions of wetting agents. The sessile bubble method has been used by Adam and Shute[4] for studying the variation of surface tension with time, of certain paraffin chain salts. The method seems to be free from contact angle effects but special precautions have to be taken against accidental contamination. Tartar, *et al.*[4a] have made a comparative study of the capillary rise and the sessile bubble methods for the determination of the variation of surface tension. They prefer the latter method and claim that it gives reproducible results.

The trough method suggested by Doss,[6] and McBain and Wilson,[7] is quite suitable for a study of the variation of surface tension with time but this method is cumbersome for the study of the variation of interfacial tension with time. The pendant drop method described by Andreas,[5] Hauser and Tucker, appears to be satisfactory for the latter purpose, but the apparatus is very complicated.

In the present method, the advantages of the pendant drop method are combined with those of the drop weight method. The method consists in forming a small drop of the solution at the end of a vertical capillary placed inside a thermostat. The drop is allowed to age, and the time required for the drop to fall, is noted. The boundary tension is calculated by applying Harkin's[8] corrections for the volume of the ideal drop.

Experimental

Reagents empolyed

(i) *Benzene.*—The benzene (Kahlbaum's pure grade) was distilled in an all-glass apparatus and the middle fraction was used.

* Part of the Thesis submitted by R. S. Subrahmanya for the M.Sc. Degree of the Mysore University.

(ii) *Congorubin.*—Congorubin was purified by the sodium acetate method of Robinson.[11] It was washed with alcohol and dried in vacuum.

(iii) *Potassium iodide, acetic acid and sodium chloride.*—A. R. quality reagents were used.

Apparatus

The stalagmometer used for the measurement of boundary tension consisted of a calibrated micro burette which had a suitable capillary tube fused on to its delivery end. The tip of the capillary was carefully ground, using fine corborundum powder,[9, 10] and finally wet talc. As pointed out by Andreas, *et al.*,[5] microscopic perfection was not necessary since the liquid tended to bridge slight irregularities. The capillary tube passed through a rubber stopper fixed to a small bottle containing benzene, so that the tip was immersed about 0·5″ below the surface of benzene. The stopper carried a sensitive thermometer and a small capillary tube, open to the atmosphere. The entire apparatus was placed in an air-thermostat at 30° C. (± 0·05°). The radius of the capillary was 0·3402 cm.

Determination of Interfacial Tension between Water and Benzene

The stalagmometer was cleaned thoroughly with warm chromic acid and finally washed with conductivity water. It was then filled with conductivity water saturated with benzene. Nc grease was employed to lubricate the stopcock. The bottle was filled with benzene saturated with water, and kept in the thermostat for five to six hours. The stopcock was gently opened and a small drop of water was allowed to form in the benzene. The drop was sucked back so that the liquid meniscus was at a fixed mark on the capillary tube. The water level in the micro burette was then noted by means of a travelling microscope. The stopcock was next opened and a fresh drop of water in benzene, was allowed to form slowly. The time of formation of each drop was about five minutes. After the drop fell off from the tip, the water was once again sucked back to the mark, and the stopcock closed. The microburette was then read and the volume of the drop determined. Within the limits of experimental error, it was noticed that the volume of the drop of water was independent of the time of formation of the drop. Evaporation of water from the microburette was minimised by attaching to its open end a fine capillary. The reproducibility in the formation of drops can be gauged from the following values obtained in an experiment:—0·3903 c.c., 0·3909 c.c., 0·3903 c.c., 0·3887 c.c.—mean value 0·3901 c.c. The interfacial tension γ was calculated from the following formula:—

$$\gamma = \frac{V(D_2 - D_1)g}{2R\phi},$$

where, R = radius of tip of capillary,

V = volume of drop,

D_2 = density of water,

D_1 = density of benzene,

g = acceleration due to gravity.

$R/V^{1/3}$ being known the value of ϕ was ascertained from data furnished by the Harkins and Brown.[8] Using the above formula, the interfacial tension was calculated. The mean value for the benzene-water interface was 34·29 dynes per cm. which agrees with the standzard value of 34·34 at 30° within the limits of experimental error (about 0·3%).

Determination of the Variation with Time of the Interfacial Tension between Benzene and Aqueous Solutions of Rubin

As pointed out already, the chief difficulty in the determination of the variation of interfacial tension with time, was the maintenance of the interface in an undisturbed condition during the entire period, over which the measurement extended. In the present investigation, this difficulty was overcome by employing the principle of the pendant drop method. The following procedure was adopted:—

After cleaning, the stalagmometer was filled with the rubin solution saturated with benzene, while the bottle was filled with benzene saturated with the rubin solution. After the attainment of temperature equilibrium, a drop of known volume was produced in four to five seconds at the end of the capillary tube. The drop was allowed to hang on at the tip of the capillary when it was noticed that the semi-spherical shape of the drop gradually changed to that of an elongated sphere until finally the drop fell into the benzene. The interval between the formation and the falling of the drop was noted. The aqueous solution was sucked back to the mark and the final volume of the drop determined. The interfacial tension at the time of falling of the drop was determined by Harkin's method, as already described. It was noticed that for a given concentration of rubin, the time of falling of a drop was a function of the volume of the drop. The intervals for the falling of drops having various volumes were noted and the corresponding values of interfacial tensions calculated. Fig. 1 represents the variation of interfacial tension with time for different concentrations of rubin solution. The rubin solution (0·005%) was then mixed with a few drops

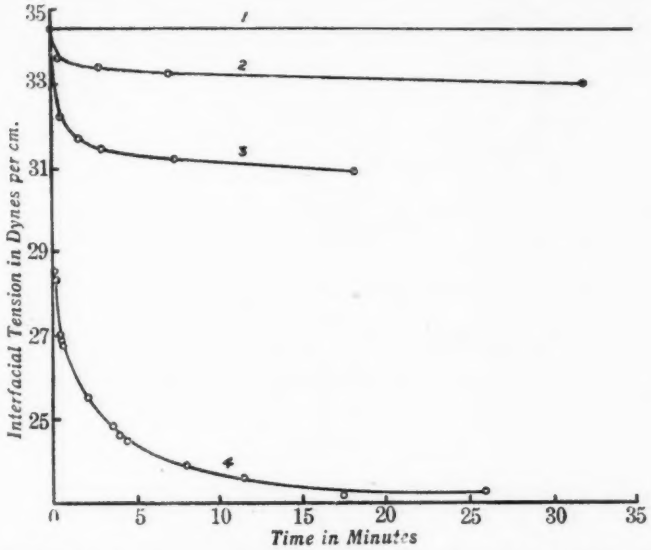

FIG. 1. Effect of concentration on the variation of interfacial tension, with time, of Congorubin solution at benzene interface.

Concentration of congorubin pertaining to curve 1 = 0·00005%, curve 2 = 0·0005%, curve 3 = 0·005%, and curve 4 = 0·05%.

of dilute acetic acid to lower the pH to 3·8 and fresh measurements made with the solution. From the results obtained (Fig. 2) it is clear that a lowering of pH greatly diminishes the interfacial tension.

Effect of Salts on the Variation of Interfacial Tension with Time

Evans[13] and Guest[14] have shown that salts of the type of sodium or potassium chloride increase the interfacial tension between aqueous solutions and an inert organic liquid, while potassium iodide decreases the tension. It was of interest to examine if sodium chloride and potassium iodide have the same effect on the interfacial tension between congorubin solution and benzene and how the interfacial tension varies with time. 0·005% rubin solution was employed. The salt concentration was 0·1 molar. The results obtained are indicated in Fig. 3. It will be noticed that both the salts considerably lower the interfacial tension, the effect being greater with the iodide. With time, the interfacial tension decreases in both the cases.

Measurement of Surface Tension

It was found necessary to prevent evaporation of water from the pendant drop, by having in the bottle some of the rubin solution, 1 to 2 mm.

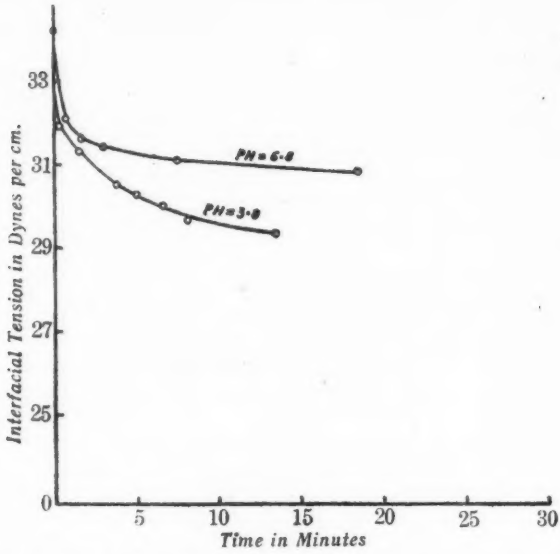

FIG. 2. Effect of pH on the variation of interfacial tension, with time, of Congorubin solution (0·005%) at benzene interface.

below the drop. The variation of surface tension with time for the rubin solution was also determined by the trough method. The results obtained by the two methods are given in Fig. 4. The agreement between the values obtained by the two methods is very satisfactory.

DISCUSSION

Variation of Surface Tension with Time

Investigations by the present method, on the variation of surface tension with time, using 0·2% solution of congorubin in water, confirm the results obtained by the trough method. The present method can be employed for a study of surface tension at different temperatures more easily than the trough method. Another advantage of the method is that only small quantities of solutions are required. The slow variation of surface tension with time shows that the accumulation of the rubin molecules at the surface of the solution is of the activated type and is a slow process (*cf.*, Doss,[15] McBain, *et al.*[16]).

Variation of Interfacial Tension with Time of Aqueous Rubin Solutions at Benzene Interface

The effect of concentration of rubin on the variation of interfacial tension with time is quite marked. At very low concentrations (0·00005%) of

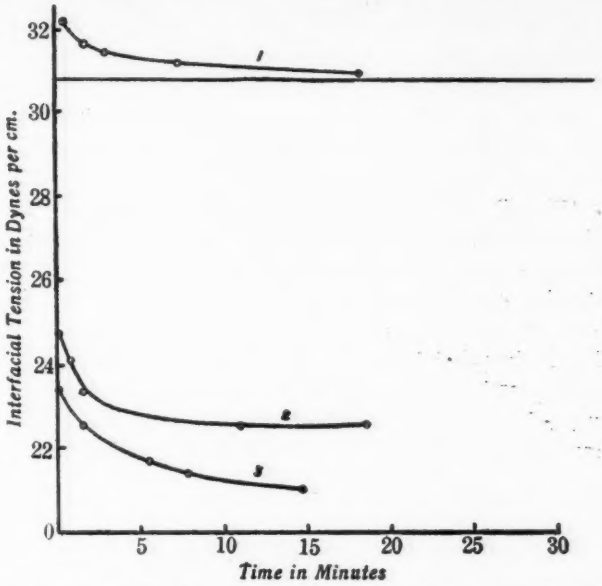

FIG. 3. Effect of Salts on the variation of interfocial tension, with time, of Congorubin solution at benzene interface.

Composition of aqueous solution :—

Curve 1 0·005% dye
" 2 " + 0·1 N sodium chloride.
" 3 " + 0·1 N potassium iodide.
" 4 0·1 N potassium iodide.

(*Note.*—As with potassium iodide solution, there was no change in interfacial tension with time, in the case of 0·1 N sodium chloride).

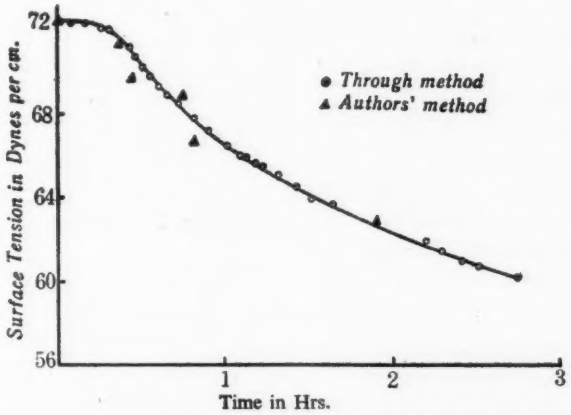

FIG. 4. Variation of surface tension with time of 0·2% Congorubin solution.

rubin, the interfacial tension will be practically the same as that between water and benzene. There is scarcely any change with time. But at concentrations of the order of 0·0005% and above there is not only a fall in the interfacial tension but also a variation in the tension with time. This change is rapid in the beginning but gradually falls off. At the air-solution interface on the other hand, there is no variation in surface tension during the first 20 minutes (Fig. 4). The tension then begins to diminish and we finally get a practically constant value which is characteristic of a condensed film. Lower concentrations ($< 0{\cdot}2\%$) of rubin cannot be employed for the study of surface tension owing to very slow accumulation. In studying interfacial tension, however, solutions of far lower concentrations (0·05%) can be used. A fall in interfacial tension with time is noticed in such solutions. The film in this case is of the gaseous type as can be gathered from the nature of the curve, while the corresponding film for the air-solution interface is of the condensed type. The difference can be explained thus:—

Congorubin has four hydrophilic groups as shown by its constitution.—

$$\begin{array}{l} C_6H_4 - N = N - [2] - C_{10}H_5 \begin{matrix}[1]\ NH_2 \\ [4]\ SO_3Na\end{matrix} \\ \quad\quad | \\ C_6H_4 - N = N - [1] - C_{10}H_5 \begin{matrix}[2]\ OH \\ [8]\ SO_3Na\end{matrix} \end{array}$$

As shown by Doss[12] for benzopurpurin, the slow surface accumulation of rubin may be due to the extra activation energy required to eject two of the hydrophilic groups into the air. Thus the activated molecule will have the hydrophobic group and also the hydrophilic group pointing out towards air. This explains the formation of the condensed film at the air-water interface. But when air is replaced by benzene there will perhaps be no tendency for the two hydrophilic groups to come out. On the other hand the hydrophilic groups will all be pointing out towards water while the hydrophobic portion will get oriented towards benzene, as in the case of sodium oleate solutions.[5] Hence the only force that retards the rate of accumulation at the benzene interface is the electrical double layer formed at the interface due to accumulation of rubin molecules. Owing to the potential of the electrical double layer, the concentration of the capillary active ion, in the region just beneath the surface layer, will be very much suppressed and will be equal to[15]

$$c \times e^{-\frac{e\psi_0 x}{kT}}$$

where c = bulk concentration of the solution,

ϵ = charge on the electron,

ψ_0 = potential due to the surface fully covered by the solute molecules,

x = fraction of the total surface covered,

k = Boltzmann constant,

T = absolute temperature.

Thus, accumulation at the surface occurs from a region of low concentration. Hence the rate of accumulation will be proportional to

$$e^{-\frac{e\psi_0 x}{kT}}.$$

Examination of this equation shows that the rate of accumulation should be very high at the start (*i.e.*, for small values of x). As the surface gets enriched with respect to the solute molecules (*i.e.*, x increasing) the rate of accumulation goes on diminishing exponentially. Thus the rate of fall in interfacial tension will be high to begin with, but rapidly diminishes with time.

Andreas[5] and others have determined the variation of surface tension with time, using sodium oleate solutions. They have also determined the variation of the interfacial tension between these solutions and mineral oil. Unlike congorubin, sodium oleate gives the gaseous type of films both at the air-water interface and at the water-mineral oil interface. Evidently, the accumulation of the sodium oleate is mainly governed by the electrical double layer at the two interfaces. Adam and Shute[4] have come to similar conclusions by working with cetyl pyridinium bromide and sodium dodecyl sulphate solutions.

The rapid fall of interfacial tension (*i.e.*, the high rate of accumulation of the rubin at the interface) in presence of electrolytes needs some explanation. Adam and Shute[4] have noticed similar effects with cetyl pyridinium bromide at the air-water interface. They state that the rapid accumulation is due to micelle formation. But the actual mechanism proposed is that the high negative charge on the micelles drives very rapidly the molecular species of the pyridinium bromide, to the interface. In the case of the congorubin solution-benzene interface the effect can be ascribed to the diminution in the value of ψ_0 (Zeta-potential) with an increase in the concentration of the electrolyte, in the rubin solutions. The rate of accumulation which is proportional to $ce^{-\frac{e\psi_0 x}{kT}}$ gets enhanced with the decrease in the value of ψ_0. Hence the interfacial tension falls rapidly when the concentration of the electrolyte is increased. The effect of pH on the variation of interfacial tension with time can also be explained on the basis of the diminution of

the zeta potential. An increase in hydrogen-ion concentration reduces the zeta potential and thus increases the rate of accumulation (Fig. 2).

SUMMARY

1. A new method for the determination of variation of interfacial and surface tensions with time, has been described. In this method, the advantages of the pendant drop method are combined with those of the drop weight method, thus simplifying the experimental technique.

2. Variation of interfacial and surface tensions with time has been investigated for congorubin solutions. The rubin solution yields at the air-liquid interface a solid film and at the solution-benzene interface a gaseous type of film.

3. The effect of concentration of rubin on the variation of interfacial tension with time has been studied. At concentrations of rubin higher than 0·0005% the fall in the interfacial tension will be large.

4. Salts like sodium chloride and potassium iodide lower considerably the interfacial tension between rubin solution and benzene. Lowering of pH also brings about a fall in interfacial tension.

5. The slow variation of interfacial tension has been accounted for, on the basis of changes in zeta-potential.

REFERENCES

1. Adam, N. K. .. *The Physics and Chemistry of Surfaces*, 2nd Edn. General.
2. Venkatachala .. *M.Sc., Thesis*, 1941, *Mys. Uni.*. p. 35.
3. Krishnappa .. *Ibid.*, 1943, *Mys. Uni.*, p. 38.
4. Adam and Shute .. *Trans. Far. Soc.*, 1938, p. 758.
4 *a*. Tartar, Sivertz and Reitmeier *J. Am. Chem. Soc.*, 1940, **62**, 2381.
5. Andreas, Hauser and Tucker.. *J. Phy. Chem.*, 1938, **42**, 1001.
6. Doss .. *Proc. Ind. Acad. Sci.*, 1936, **4**, 97.
7. McBain and Wilson .. *J. Amer. Chem. Soc.*, 1936, **58**, 379.
8. Harkins and Brown .. *Ibid.*, 1919, **499**.
9. Eversole and Dallas S. Dedrick *J. Phy. Chem.*, 1933, 1205.
10. Dallas and Maurice H. Hanson *Ibid.*, 1933, 1215.
11. Doss .. *Kolloid Z.*, 1938, **84**, 138.
12. ———— .. *Ibid.*, 1939. **87**, 272.
13. Evans .. *Trans. Far. Soc.*, 1937, **33**, 794.
14. Guest .. *Proc. Roy. Soc.*, 1939, **170 A**, 501,
15. Doss .. *Kolloid Z.*, 1939, **86**, 205.
16. McBain, Ford, Mills .. *J. Am. Chem. Soc.*, 1940, **62**, 1319,

X-RAY ANTI-REFLECTIONS IN CRYSTALS

By G. N. Ramachandran, F.A.Sc. and Gopinath Kartha
(Department of Physics, Indian Institute of Science, Bangalore-3)

Received January 21, 1952

1. Introduction

This paper deals with the theory of some interesting phenomena which are observed in the transmitted X-ray beam when a Bragg reflection takes place in a crystal. Obviously, if the crystal is non-absorbing, then the whole of the incident energy must be transmitted in the absence of the Bragg reflection and when a reflection occurs, the energy which is reflected will manifest itself as a reduction in the intensity of the transmitted beam. Thus, the reflected and transmitted intensities would be complementary, so that if R and T are the reflection and transmission coefficients, then

$$R + T = 1. \tag{1}$$

If the crystal is absorbing, we have one more mechanism whereby energy may be abstracted from the incident beam. If A is the fraction of the incident intensity removed in this way, we have from *a priori* considerations, the following equation:

$$R + T + A = 1 \text{ or } R + T = 1 - A = T_0 \text{ (say)} \tag{2}$$

This means that T is always less than or equal to T_0, and near the Bragg reflection, when R has an appreciable value, there should be a reduction in the transmitted intensity.

The foregoing deduction is, however, based on the idea that absorption and reflection are independent processes. However, if one supposes that the two are interrelated and that the absorption coefficient can itself be modified by the presence of an interference maximum, then conditions may be different. Thus, if the effective absorption coefficient is reduced for directions of incidence close to the Bragg angle, then the quantity A in Eqn. (2) would itself be reduced and one cannot conclude, without further calculations, whether the transmission would effectively decrease or increase. It is conceivable that the decrease in absorption coefficient would be such that the consequent increase in the transmited intensity may be larger than the decrease due to part of the energy being reflected. In such a case, one may expect a peak in the transmitted beam near the Bragg reflection rather than a dip. In fact, such a result has been observed by Campbell (1951)

using perfect calcite crystals. He found that the peak of the transmitted intensity may even be several hundred times as large as T_0. The name "anti-reflection" is suggested for this phenomenon. As is evident from the above discussion, such a phenomenon can be expected only with an absorbing crystal. If there is no absorption, Eqn. (1) would be rigorously valid and there would be always a diminution in T near a Bragg reflection. Also, the greater the value of A, *i.e.*, the thicker the crystal, the more striking would be the intensity changes produced by a small alteration in the absorption coefficient, and consequently the more prominent would be the anti-reflection peak.

These qualitative arguments are borne out by the detailed theory given below. It is based on the well-known dynamical theory of Ewald (1916). In particular, the development of the theory due to Laue (1949) forms a proper starting point for the discussion in this paper. Compact expressions have been derived for T and R, both in the so-called "Laue" and "Bragg" cases, and these have been numerically worked out in the former case. They show clearly that, for increasing thicknesses of the crystal, the transmission curve slowly alters its form from a minimum to a sharp maximum near the Bragg reflection.

2. PREVIOUS LITERATURE

On the experimental side, the subject goes back to an interesting observation made by Rutherford and Andrade (1914) during their determinations of γ-ray wavelengths using crystal diffraction. They observed in general a diminution in the intensity of the transmitted beam when a diffracted beam occurred. However, this diminution was not observed when a good perfect crystal was chosen for the experiment. In continuation of this experiment, Borrmann (1941) allowed a divergent beam of X-rays to fall on a crystal plate of quartz (0.2 mm. thick) and found lines in the transmitted beam where the transmission was appreciably reduced. However, when he chose a perfect crystal, as evidenced by the sharpness of the X-ray reflection, he found that the lines exhibited a "*Helldunkelstruktur*", *i.e.*, adjoining areas having an intensity larger and smaller than the general background. The occurrence of a transmitted beam of intensity larger than T_0 is particularly noteworthy.

Lonsdale (1947) made similar studies with a number of crystals and confirmed Rutherford and Andrade's observation. She found that the deficiency lines in the transmitted beam were imperceptible with a perfect crystal, while they became clearer with increasing degree of mosaicity. She did not make a critical study of the distribution of intensity of these lines,

Making use of the dynamical theory of X-ray diffraction, Laue (1949) has worked out the theory of the transmission of X-rays when interference takes place. In particular, he considered the so-called " Laue case ", *i.e.*, when both the incident and diffracted beams emerge from the back surface of the crystal plate. Using his formulæ he also calculated numerically the angular distribution of intensity of the reflected and transmitted beams in a few particular cases. These are similar to those observed by Borrmann (1941), although no quantitative comparison can be made.

More recently, Campbell (1951 *a*, *b*) studied the phenomenon quantitatively, using Geiger-Müller counters. The experiments were performed with a monochromatised beam of Cu Kα having a small angle of divergence of the order of 15 seconds of arc. Symmetrical " Laue " reflections were obtained from the crystal under study and both the reflected and the transmitted intensities were measured simultaneously for different settings near the Bragg reflection by means of two Geïger counters. Sharp *maxima* were found *both* in the reflected and the transmitted beams with perfect crystals. With an imperfect crystal, the increase was imperceptible, but there was no decrease. Campbell has stated in his paper (1951 *b*) that the sharp maxima in the transmitted beam do not correspond to the curves given in Laue's paper (1949) and that his results are therefore inexplicable on this theory. However, the conditions of his experiment are different from those assumed in the theory and when the proper conditions are incorporated in the theory, it leads to sharp maxima, as is shown below.

3. Notation

The notation follows mainly Laue's symbology (1949), although a number of new symbols are used. Zachariasen (1945) has also given an account of the dynamical theory and his notation has been adopted in certain cases. The symbols within brackets are the equivalents in Zachariasen's notation of those used here.

λ	Wavelength of the X-rays in vacuum	(λ_0)
k	($= 1/\lambda$), length of the wave-vector in vacuum	(k_0)
h	Index (subscript) denoting a particular X-ray reflection (This index may be omitted when there is no confusion).	(H)
θ	Angle of incidence	(θ)
θ_G	Geometrical Bragg angle	(θ_B)
θ_B	Bragg angle, allowing for refraction	
μ	Linear absorption coefficient (in the absence of Bragg reflection)	(μ_0)

D	Thickness of the crystal	(t)
C	Polarisation factor, = 1 for the normal component and = cos 2 θ for the parallel component	(K)
γ_0, γ_h	Cosines of the angles made by the incident and reflected beams respectively with the normal to the surface	(γ_0), (γ_H)
χ_0, χ_h	Fourier components of order 0 and h in the triple Fourier expansion of $4\pi\alpha$, where α is the polarisability	(ψ_0), (ψ_H)
χ_{hr}, χ_{hi}	Real and imaginary parts of χ_h: $\chi_h = \chi_{hr} + i\chi_{hi}$	(ψ_H'), (ψ_H'')
$\mathbf{D}_0$, $\mathbf{D}_h$	Electric vectors of the diffracted waves of order 0 and h	($\bar{D}_0$), ($\bar{D}_H$)
D_0, D_h	Magnitudes of $\mathbf{D}_0$, $\mathbf{D}_h$	(D_0), (D_H)
z	Unit vector, normal to the surface, directed inside the crystal	($\bar{n}$)
$\mathbf{R}_0$, $\mathbf{R}_h$	Wave vectors, of order 0 and h inside the crystal	($\bar{k}_0^B$), (k_H^B)
1, 2	Subscripts to denote the two wave fields inside the crystal	($'$), ($''$)
a, d	Superscripts, a to denote the front, and d the back surface of the crystal, *e.g.* $D_0^{(a)}$ represents the electric vector of the incident beam	(^{0}), (^{e})
α_h	$= (\sin 2\theta_G)(\theta - \theta_G)$	($\alpha/2$)
β_h	$= 2\alpha_h - \chi_0(1 - \gamma_h/\gamma_0)$	($2z/b$)
β_r	Real part of β_h, $= 2\alpha_h - \chi_{0r}(1 - \gamma_h/\gamma_0)$	
y	$= \beta_r/2C \left[\frac{\gamma_h}{\gamma_0} \chi_h \chi_{\bar{h}}\right]^{\frac{1}{2}}$	(y)
R, T	Reflection and transmission coefficients	
T_0	Transmission coefficient in the absence of reflection. $= \exp(-\mu D)$.	

4. DYNAMICAL THEORY OF X-RAY REFLECTION

The dynamical theory, in its most general form, seeks to determine the interaction of a crystal with an incident beam of radiation and to work out the phenomena which accompany this interaction. Here, we are interested in the case when the wavelength is of the same order as the lattice spacing of the crystal, and in particular when there is only one diffracted ray. The

fundamental equations in this case are:

$$\left.\begin{aligned}\frac{R_0^2 - k^2}{R_0^2} D_0 &= \chi_0 D_0 + \chi_{\bar{h}} C D_h \\ \frac{R_h^2 - k^2}{R^2} D_h &= \chi_0 D_h + \chi_h C D_0\end{aligned}\right\} \quad (3)$$

Putting

$$R_0 = (1 + \delta_0)\, k \text{ and } R_h = (1 + \delta_h)\, k,$$

where δ_0, $\delta_h \ll 1$, one obtains the following equation as a condition for the compatibility of the two equations in (2):

$$4\delta_0\delta_h - 2\chi_0(\delta_0 + \delta_h) + C^2\chi_h\chi_{\bar{h}} - + \chi_0^2 = 0.$$

We are specially interested in settings close to the Bragg angle. When a setting is specified, then there is a definite relation between the incident and the diffracted rays, and therefore δ_0 and δ_h are also related. Thus, the equation mentioned above becomes a quadratic in δ_0 alone (or in δ_h alone), giving two roots for δ_0. Corresponding to each value of δ_0, one obtains a value of D_h/D_0 for a particular setting and thus there are two wave fields inside the crystal, into which the incident beam is split. To calculate the transmitted or the diffracted wave outside the crystal, these two wave fields have again to be summed up on emergence from the crystal.

In the application of the dynamical theory to the X-ray reflection from a parallel crystal plate, two cases arise according as the diffracted beam emerges from the same face as, or the opposite face to, that on which X-rays are incident. These two cases are commonly referred to as the "Bragg" case and the "Laue" case respectively. However, a different nomenclature is called for, since the term "Bragg reflection" occurs often in connection with this subject and should not be confused with the reflection in the Bragg case. Further, it is also common to use "Laue reflection" to mean crystal reflection of *white* X-rays and "Bragg reflection" for reflection of *monochromatic* X-rays. In view of these, the terms "surface reflection" and "internal reflection" are suggested to refer to the two cases when the reflected X-rays come out of the same surface on which the incident X-rays strike and when the reflected X-rays pass through the thickness of the crystal, respectively.

If we denote by D_{01} and D_{02} the magnitude of the electric vectors in the transmitted beam corresponding to the two wave-fields 1 and 2, and by D_{h1} and D_{h2} the corresponding quantities in the diffracted beam (of order h) then the boundary conditions in the two types of reflection will be for an internal reflection

$$D_{01} + D_{02} = D_0^{(a)};\ D_{h1} + D_{h2} = 0 \quad (4)$$

and for a surface reflection,

$$D_{01} + D_{02} = D_0^{(a)};$$

$$D_{h1} \exp\left[-2\pi i\,(\mathbf{R}_{h1}\cdot\mathbf{z})\,D\right] + D_{h2} \exp\left[-2\pi i\,(\mathbf{R}_{h2}\cdot\mathbf{z})\,D\right] = 0. \quad (5)$$

where $\mathbf{z}$ is a unit vector along the direction of the thickness. The quantities to be determined in each case, are

for an internal reflection

$$\left.\begin{aligned} D_{01} \exp\left[-2\pi i\,(\mathbf{R}_{01}\cdot\mathbf{z})\,D\right] + D_{02} \exp\left[-2\pi i\,(\mathbf{R}_{02}\cdot\mathbf{z})\,D\right] &= D_0^{(d)} \\ D_{h1} \exp\left[-2\pi i\,(\mathbf{R}_{h1}\cdot\mathbf{z})\,D\right] + D_{h2} \exp\left[-2\pi i\,(\mathbf{R}_{h2}\cdot\mathbf{z})\,D\right] &= D_h^{(d)} \end{aligned}\right\} \quad (6)$$

and for a surface reflection

$$\left.\begin{aligned} D_{01} \exp\left[-2\pi i\,(\mathbf{R}_{01}\cdot\mathbf{z})\,D\right] + D_{02} \exp\left[-2\pi i\,(\mathbf{R}_{02}\cdot\mathbf{z})\,D\right] &= D_0^{(d)} \\ D_{h1} + D_{h2} &= D_h^{(a)} \end{aligned}\right\} \quad (7)$$

5. Expressions for R and T in the Case of Internal Reflection

Laue (1949) has considered this case. The formulæ (8) and (9) given below can readily be derived from his equations. Here, they have been put in a form convenient for numerical computation. Further, the rapidly varying cosine function in Laue's formulæ have been neglected, as these only represent interference bands, which arise from interference between the two surfaces of the crystal plate. These bands would be very closely spaced, the number between two successive orders of Bragg reflection being of the order of D/λ, which is about 100,000 even with a crystal 0·01 mm. thick and even more with thicker crystals. Even a variation of the order of λ in the thickness of the crystal would obliterate them. It is therefore justifiable to neglect these fine variations of intensity and to take an average. Eqn. (8) and (9) represent in fact such an average value for the intensity.

$$R = \left|\frac{\chi_h}{\chi_{\bar{h}}}\right| \frac{\exp\left\{-\tfrac{1}{2}\left(\frac{1}{\gamma_0} + \frac{1}{\gamma_h}\right)\mu D\right\}}{2\cosh^2 v_r} \cosh 2\eta D \quad (8)$$

$$T = \frac{\exp\left\{-\tfrac{1}{2}\left(\frac{1}{\gamma_0} + \frac{1}{\gamma_h}\right)\mu D\right\}}{2\cosh^2 v_r} \cosh 2(\eta D + v_r) \quad (9)$$

where

$$\sinh v_r = \beta_r / 2C \left[\frac{\gamma_h}{\gamma_0}\chi_h\chi_{\bar{h}}\right]^{\frac{1}{2}} \quad (10)$$

and

$$\eta = \frac{\tfrac{1}{4}\left(\frac{1}{\gamma_0} - \frac{1}{\gamma_h}\right)\beta_r\mu}{\left(\beta_r^2 + 4C^2\frac{\gamma_h}{\gamma_0}\chi_h\chi_{\bar{h}}\right)^{\frac{1}{2}}} + \frac{\frac{C^2}{\gamma_0}\chi_{hr}\chi_{hi}\pi k}{\left(\beta_r^2 + 4C^2\frac{\gamma_h}{\gamma_0}\chi_h\chi_{\bar{h}}\right)^{\frac{1}{2}}} \quad (11)$$

In these equations, β_r is a measure of the departure of the glancing angle θ from the Bragg angle θ_B, *i.e.*, $\beta_r = 0$ corresponds to $\theta = \theta_B$.

It is interesting to note the following deductions which readily follow from eqns. (8) and (9):

(*a*) When $|\beta_r| \gg 2C \left[\frac{\gamma_h}{\gamma_0} \chi_h \chi_{\bar{h}}\right]^{\frac{1}{2}}$, *i.e.*, for directions sufficiently remote rom the Bragg angle,

$$R = 0 \text{ and } T = \exp(-\mu D/\gamma_0) = T_0 \tag{12}$$

as should be the case. This obvious result has been particularly mentioned here, because the curves in Laue's paper may lead to an erroneous impression that T increases with β_r on one side of the maximum. His curves I and II in Figs. 2 (*a*), (*b*), (*c*) have been drawn without taking into account the $\cosh^2 v_r$ in the denominator of Eqns. (8) and (9) above. When this is also included, the above result (12) follows

(*b*) when $\beta_r = 0$

$$T = \left|\frac{\chi_h}{\chi_{\bar{h}}}\right| R = \tfrac{1}{2} \exp - \mu D \left[\tfrac{1}{2}\left(\frac{1}{\gamma_0} + \frac{1}{\gamma_h}\right) - \frac{C}{\sqrt{\gamma_0 \gamma_h}} \frac{\chi_{hi}}{\chi_{0i}}\right]. \tag{13}$$

Thus, for a crystal obeying Friedel's Law, R = T at the peak of the reflection, as has already been pointed out by Laue.

It is interesting to note that the ratio R/T_0 depends on the ratio χ_{hi}/χ_{0i}, *i.e.*, on the ratio of the *imaginary components* of the structure factors of order h and zero. This ratio would correspond to the F-value, *i.e.*, the ratio of the real components, for wavelengths sufficiently far away from absorption frequencies. If this is not so, then the peak intensity of an internal reflection does not represent the structure factor of the crystal.

Since $\chi_{hi} \leqslant \chi_{0i}$ and $C \leqslant 1$, R cannot exceed the value $\frac{1}{2}$ for a symmetrical internal reflection. This is to be expected, because for a non-absorbing crystal, $R = \frac{1}{2}$ at the peak.

(*c*) For intermediate values of β_r, it is convenient to introduce the quantity $y = \sinh v_r$, so that

$$\eta = \mu \left[\tfrac{1}{4}\left(\frac{1}{\gamma_0} - \frac{1}{\gamma_h}\right) \frac{y}{\sqrt{1+y^2}} + \tfrac{1}{2} \frac{C}{\sqrt{\gamma_h \gamma_0}} \frac{\chi_{hi}}{\chi_{0i}} \frac{1}{\sqrt{1+y^2}}\right] \tag{14}$$

Also, we have

$$\cosh^2 v_r = (1 + y^2) \tag{15}$$

From the above definition, $y \propto \beta$ and hence to $(\theta - \theta_B)$, and units of y may thus be employed as abscissæ in plotting the variation of R and T with glancing angle, as has been done by Zachariasen (1945). $y = 1$ would

correspond to a value of $(\theta - \theta_B)$ equal to the half-width of the corresponding surface reflection curve if the crystal is non-absorbing (*i.e.*, for the same reflection, h). As is well known this is of the order of a few seconds of arc, and its magnitude can be readily calculated from θ and the structure factor, so that the y-unit forms a convenient unit for representing reflection curves.

6. Calculation of Reflection and Transmission Curves for Internal Reflections

Laue (1949) has plotted the variation of R and T with angle θ for the 111 and 200 reflections of rock-salt, with thicknesses of the order of 0·1 mm. and using Cu K_α radiation. He obtained curves, which exhibit variations similar to those observed by Borrmann (1941), namely, an increase and decrease of intensity compared to the background on either side of the Bragg reflection. The exponent $(\mu D/\gamma)$ is of the order of 1·0 to 2·0 and is of the same order of magnitude as that employed by Borrmann, who used quartz crystals 0·2 mm. thick and Fe K_α rays. In Campbell's experiments (1951 *b*) on the other hand, calcite crystals, 0·4 to 1·00 mm. thick were used with Cu K_α, for which $\mu D/\gamma \sim 8$ to 20. The conditions in the experiments of Campbell are not therefore comparable with those assumed in Laue's calculations, and it is not surprising that the latter do not correspond to the observations of Campbell. Consequently, the authors have plotted a series of reflection and transmission curves, with varying $(\mu D/\gamma)$, for $(10\bar{1}\cdot1)$ reflection of calcite, when the crystal is cut with its surfaces perpendicular to the lattice planes concerned.

For convenience, we write $P = \mu D/\gamma$, and a series of curves have been plotted for values of P = 0, 0·5, 1·0, 1·5, 2, 3, 4, 6, 8, 20. As mentioned in the last section, the abscissæ are marked in y-units, $y = 1$ actually corresponding to 3·6″ of arc in this case. The relevant data required for the calculation have been taken from Zachariasen (1945) and are:

$$\mu = 183 \text{ cm.}^{-1} \qquad \gamma_0 = \gamma_k = 0{\cdot}967$$

$$\chi_{0r} = -17{\cdot}44 \times 10^{-6} \qquad \chi_{0i} = -0{\cdot}448 \times 10^{-6}$$

$$\chi_{hr} = -8{\cdot}57 \times 10^{-6} \qquad \chi_{hi} = -0{\cdot}429 \times 10^{-6}$$

The curves in Figs. 1 and 2 correspond only to the normally polarised component (C = 1). Since μ and γ are fixed quantities for the different curves, varying values of P correspond to varying thicknesses D, which may be readily calculated, since $\mu/\gamma = 189$.

The curve for P = 0 is hypothetical, for with an absorbing crystal $(\mu \neq 0)$, P can become zero only if the thickness D vanishes. Actually, eqns. (8) and (9) from which the curves have been plotted assumes that the

thickness of the crystal is large enough compared with the lattice spacing. However, this particular curve may be said to correspond to the case when the crystal becomes non-absorbing, other conditions remaining the same. All the other curves relate to crystals of varying thickness D.

The following are clear from these curves. Considering first Fig. 1 (reflection), all the curves are symmetrical about the ordinate for the peak. The peak intensity steadily decreases with increasing thickness, but the decrease is far less rapid than the corresponding decrease of T_0. Thus, for $P = 0$, the peak is $0{\cdot}5$ ($T_0 = 1$); this decreases only to about $0{\cdot}23$ for $P = 2$, when the transmitted beam has dropped to $0{\cdot}135$. Thereafter the decrease in the peak intensity of the reflected beam is much less rapid. In fact for $P = 20$, for which T_0 will only have a value of the order of 10^{-9}, the peak reflection is as large as $0{\cdot}1$, *i.e.*, about a hundred million times the transmitted intensity for settings away from the Bragg reflection.

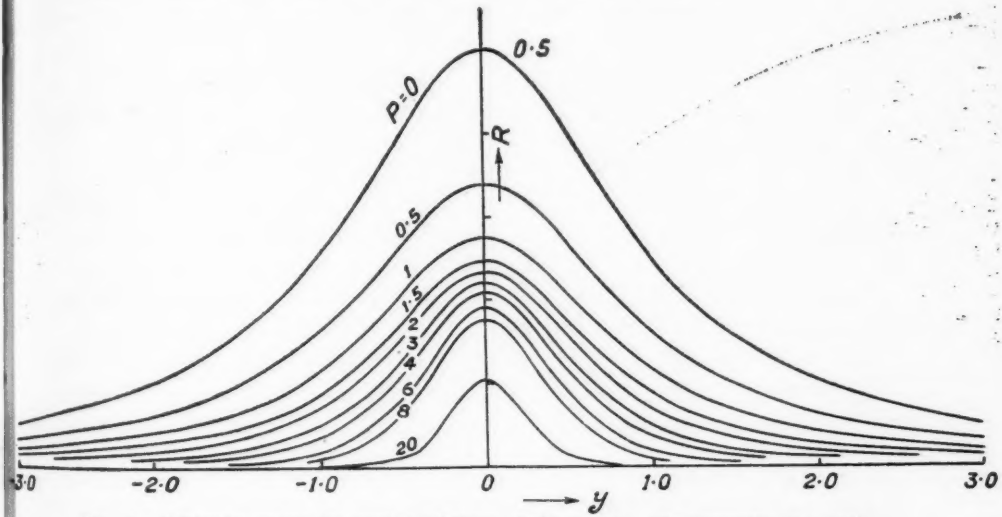

FIG. 1. Reflection curves for varying thickness of the crystal. The parameter $P = \mu D/\gamma$.

The variations in the intensity of the transmitted beam predicted by the theory is even more interesting. For $P = 0$ obviously the transmission curve (Fig. 2) is complementary to the reflection curve and exhibits only a minimum. However, for small finite values of P (*i.e.*, for small thicknesses), it exhibits both a minimum and a maximum and the intensity distribution is asymmetric about the peak of the Bragg reflection (*i.e.*, $y = 0$). On approaching the Bragg setting from the left, the transmitted intensity first becomes less than the normal value (T_0), then it rises and becomes larger

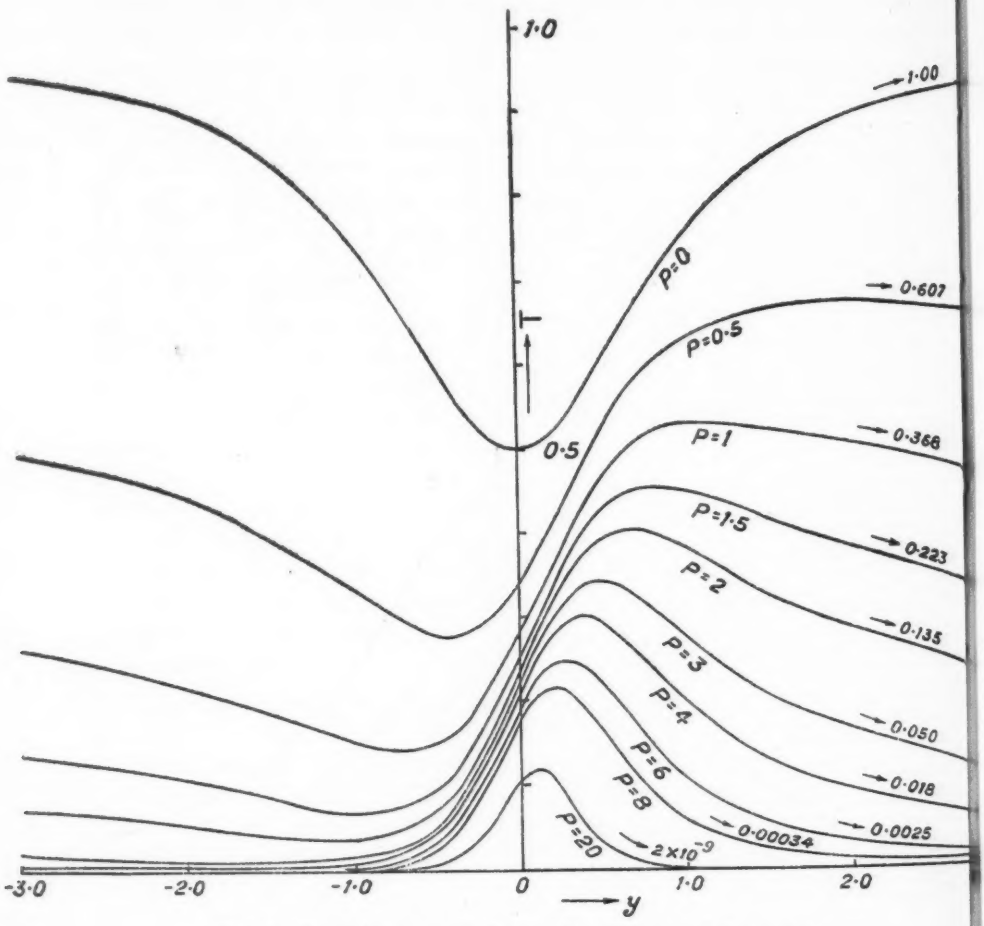

FIG. 2. Transmission curves for varying thickness of the crystal.

than the normal value, finally falling back to T_0. For small values of P, *i.e.*, very thin crystals, the decrease predominates, while with increasing thickness, the increase becomes larger and larger, until at $P = 2$ the increase is larger than the decrease. For still thicker crystals the minimum is imperceptible and only a peak is observed in the transmitted beam. It is interesting to note that the peak intensity of the transmitted beam is of the same order as that of the reflected beam, although the two peaks do not coincide. This is clearer from Fig. 3, which is discussed below. Thus,

for $P = 20$, which would correspond approximately to 1 mm. of calcite, the peak value of T is several million times the value of T_0.

We shall now consider how the theory fits the observations of Campbell. For this purpose, Fig. 3 has been drawn to correspond to Fig. 6 of his

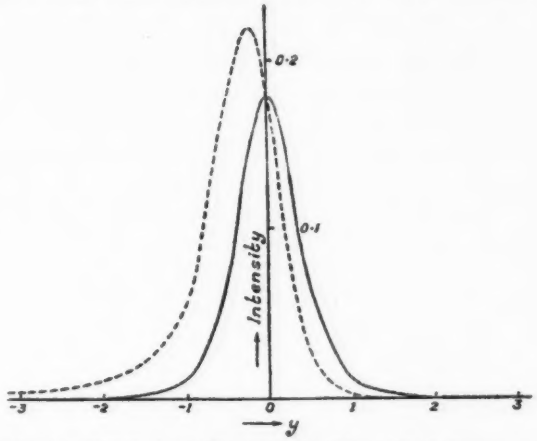

FIG. 3. Reflection (full line) and Transmission (dotted line) Curves of a crystal of calcite 0·4 mm. thick. $y = 1$ corresponds to 3·6″ of arc.

paper (1951 *b*), namely, for a crystal of calcite of thickness 0·4 mm. It is obvious at once that the theory qualitatively explains his observations (*a*) that *both* the reflected and transmitted beams exhibit sharp maxima rising up to several times above the background, (*b*) that the peak intensities of the two are nearly equal to each other and (*c*) that the peaks are extremely sharp. However, quantitative agreement is not to be expected because the theoretical curve is for an incident beam of negligibly small divergence, while in the experiment, it had a divergence of the order of 15″ of arc, which is larger than the theoretical width of the reflection or transmission curves. Because of this, the observed curves would be much broader than what is predicted by theory and the peak intensity would also be lower. When these are taken into account, the agreement between theory and experiment must be considered good.

As is clear from Fig. 3, the peaks in the reflected and transmitted beams do not coincide. Campbell (1951 *b*) did observe such an effect, but he attributed it to a mis-setting of the crystal. More careful experiments should be made to verify whether such an effect is really present or not.

The curves also show that the peak in the transmitted beam is not likely to be observed unless the incident beam has a small divergence. If

it has a large divergence, the effect would only be an average over a range of angles. This may lead to a net increase or decrease in the transmitted intensity over the background according to the thickness of the perfect crystal. For very thin crystals, it is a decrease and changes to an increase for thicker crystals. This explains the observation of Lonsdale (1947) that the deficiency lines observed by her with mosaic crystals became less clear and sometimes vanished with perfect crystals. She studied mostly crystals of low absorption (diamond and other organic crystals), for which $P \sim 1$ to 2 with a thickness of the order of a few millimetres. Consequently, if the whole crystal were perfect, there would be practically no reduction or increase in T, while if it is mosaic, a reduction would be observed. Of course, the above curves relate to calcite $10\bar{1}\cdot 1$ reflection and the conditions would be different with the crystals studied by Lonsdale (1947), but the orders of magnitude are not likely to be different. The authors have undertaken a theoretical study of the variation of R and T with various factors such as the structure factor, absorption coefficient, etc., and this would throw further light on the subject.

7. Expressions for R and T in the Case of Surface Reflection

As mentioned earlier, although Kohler (1933) has considered this case, he has made some approximations, *e.g.*, neglecting one of the two wavefields in the crystal, as it has a large attenuation coefficient. It is, however, unnecessary to make the approximation and we shall give below a brief derivation of the formulæ, both for the reflection and transmission coefficients, following closely the method and nomenclature of Laue (1949).

In the Bragg case, γ_h/γ_0 is negative and where necessary this will be denoted explicitly by writing it as $-|\gamma_h/\gamma_0|$.

Let

$$\beta = 2\alpha_h - \chi_0(1 - \gamma_h/\gamma_0)$$

Analogous to eqns. (29), (30), (31) of Laue (1949), we obtain

$$\left(\frac{D_h}{D_0}\right)_{1,2} = \left(\frac{\chi_h}{\chi_{\bar{h}}}\left|\frac{\gamma_0}{\gamma_h}\right|\right)^{\frac{1}{2}} e^{\mp u}, \tag{10}$$

where

$$\cosh u = \frac{\beta}{2C}\left[\left|\frac{\gamma_h}{\gamma_0}\right| \chi_h \chi_{\bar{h}}\right]^{\frac{1}{2}}. \tag{11}$$

We have the boundary conditions

$$D_{01} + D_{02} = D_0^{(a)};$$

$$D_{h1}\exp\left[-2\pi i\,(\mathbf{R}_{h1}\cdot \mathbf{z})\,D\right] + D_{h2}\exp\left[-2\pi i\,(\mathbf{R}_{h2}\cdot \mathbf{z})\,D\right] = 0. \tag{12}$$

and we have to determine the quantities

$$D_h^{(a)} = D_{h1} + D_{h2};$$

$$D_0^{(d)} = D_{01} \exp\left[-2\pi i\,(\mathbf{R}_{01}\cdot\mathbf{z})\,D\right] + D_{02} \exp\left[-2\pi i\,(\mathbf{R}_{02}\cdot\mathbf{z})\,D\right] \quad (13)$$

where $\mathbf{z}$ is a unit vector in the direction of the thickness D. If we write

$$\mathbf{R}_{01,2} = \mathbf{R}_0^{(a)} - k\delta_{1,2}\,\mathbf{z}, \quad (14)$$

where $\delta_{1,2}$ have the values [from Laue, 1949, Eqn. (21)]

$$\delta_{1,2} = -\tfrac{1}{2}\frac{\chi_0}{\gamma_0} + \frac{\beta}{4\gamma_h} \pm \frac{1}{4\gamma_h}\left[\beta^2 + 4C^2\frac{\gamma_h}{\gamma_0}\chi_h\chi_{\bar{h}}\right]^{\frac{1}{2}}. \quad (15)$$

Then, from eqns. (12), we have

$$D_{01} = \frac{\exp(u+x)}{2\sinh(u+x)}\,D_0^{(a)};\quad D_{02} = -\frac{\exp-(u+x)}{2\sinh(u+x)}\,D_0^{(a)}, \quad (16)$$

where

$$x = -\pi ikD\,(\delta_1 - \delta_2). \quad (17)$$

Substituting in eqns. (13), we obtain

$$R = \left|\frac{\chi_h}{\chi_{\bar{h}}}\right|\left|\frac{\sinh x}{\sinh(u+x)}\right|^2 \quad (18)$$

$$T = \left|\exp - 2\pi ikD\left(\frac{1}{\gamma_0} - \frac{\delta_1+\delta_2}{2}\right)\right|^2 \cdot \left|\frac{\sinh u}{\sinh(u+x)}\right|^2. \quad (19)$$

Unlike the Laue case, it is not possible to put eqns. (18) and (19) in terms of real quantities alone. This is so because u (and x) may be predominantly real (*i.e.*, real part $\gg$ imaginary part) for certain values of y and predominantly imaginary for other values.*

When the reflection is symmetric, *i.e.*, it takes place from lattice planes parallel to the surface, and if Friedel's law holds (*i.e.*, $|\chi_h| = |\chi_{\bar{h}}|$), then eqns. (18) and (19) reduce to

$$R = \left|\frac{\sinh x}{\sinh(u+x)}\right|^2 \qquad T = \left|\frac{\sinh u}{\sinh(u+x)}\right|^2 \quad (20)$$

These may be compared with the corresponding expressions obtained by one of the authors (Ramachandran, 1942, 1944) for a finite parallel-sided crystal plate having n lattice planes parallel to its surface. The latter are

$$R = \left|\frac{\sinh n\beta}{\sinh(\alpha+n\beta)}\right|^2 \qquad T = \left|\frac{\sinh\alpha}{\sinh(\alpha+n\beta)}\right|^2. \quad (21)$$

It is clear that there is an exact correspondence between the two, and an examination of the significance of the quanitties α and $n\beta$ in eqns. (21)

* *e. g.*, when there is no absorption, u is pure imaginary for $-1 < y < +1$ and completely real for values of y outside these limits.

shows that they are the same as u and x. This again confirms the statement made by Ramachandran (1948) that the Ewald and Darwin methods lead to identical results, in spite of their apparently very different mathematical approaches.

SUMMARY

The paper deals with the theory of an interesting phenomenon (which has been designated as "anti-reflection") that the intensity of the transmitted beam may exhibit a peak larger than the background when a Bragg reflection occurs in an absorbing crystal. The theory is based on the dynamical theory of Ewald and Laue. It comes out that the effect is due to a decrease in the effective absorption coefficient of the crystal near the Bragg reflection, and to the consequent increase in the transmitted intensity predominating over the loss of energy by reflection. The anti-reflection peak becomes more prominent, the greater the thickness of the crystal. The results of the theory are found to be in accord with the previous observations of Borrmann and Campbell. The theory further predicts that the peaks in the reflected and transmitted beams would not be coincident and this requires further verification.

REFERENCES

1. Borrmann, G. .. *Phys. Z.*, 1941, **42**, 157.
2. Campbell, H. N. .. *Acta. Cryst.*, 1951 *a*, **4**, 180.
3. ———— .. *J. App. Phys.*, 1951 *b*, **22**, 1139.
4. Ewald, P. P. .. *Ann. d. Phys.*, 1916, **49**, 1, 117.
5. Kohler, M. .. *Ibid.*, 1933, **18**, 265.
6. Laue, von M. .. *Acta Cryst.*, 1949, **2**, 106.
7. Lonsdale, K. .. *Phil. Trans. Roy. Soc.* 1947, **240, A**, 219.
8. Ramachandran, G. N. .. *Proc. Ind., Acad. Sci.* 1942, **16, A**, 336.
9. ———— .. *Ibid.*, 1944, **20**, 100.
10. ———— .. *Acta. Cryst.*, 1948, **1**, 155.
11. Rutherford, E. and Andrade, E. N. da C. *Phil. Mag.*, 1914, **28**, 263.
12. Zachariasen, W. H. .. *Theory of X-Ray Diffraction in Crystals*, 1945, New York, Wiley.

188-52 Printed at The Bangalore Press, Mysore Road, Bangalore City, by G. Srinivasa Rao, Superintendent and Published by The Indian Academy of Sciences, Bangalore